Wheel–Rail Impact Loads and Track Settlement in Railway Crossings

XIN LI

THESIS FOR THE DEGREE OF DOCTOR OF PHILOSOPHY IN SOLID AND
STRUCTURAL MECHANICS

Wheel–Rail Impact Loads and Track Settlement in Railway Crossings

XIN LI

Department of Mechanics and Maritime Sciences

CHALMERS UNIVERSITY OF TECHNOLOGY

Gothenburg, Sweden 2019

Cover:
Picture of a railway crossing in Skåne (Sweden) taken by Dr Björn Pålsson

Wheel–Rail Impact Loads and Track Settlement in Railway Crossings
Thesis for the degree of Doctor of Philosophy in Solid and Structural Mechanics
XIN LI
Department of Mechanics and Maritime Sciences
Chalmers University of Technology

Abstract

Turnouts (Switches & Crossings, S&C) are critical components of a railway track requiring regular maintenance and generating high life cycle costs. A main driver for the high maintenance costs is the need to repair and replace switch rails and crossings as these components are subjected to a severe load environment. Dynamic wheel–rail contact forces with high magnitudes are often generated in the switch and crossing panels due to the discontinuities in rail profiles, resulting in a degradation of track geometry. One critical contribution to the track geometry degradation is track settlement. It is a phenomenon where the horizontal level of the ballasted track substructure decreases in height over time when subjected to traffic loading. Due to the design of the turnout and the variation in track support conditions, the load transferred into the track bed is not uniform and the resulting variation in settlement leads to irregularities in track geometry. Poor quality in track geometry induces higher dynamic wheel–rail contact forces and increases the degradation rate resulting in further differential track settlement, and possibly increased wear, plastic deformation and rolling contact fatigue of the rails. Thus, it is important to understand how settlement evolves under repeated loading to support product development and maintenance procedures of S&C, to provide a more uniform load distribution on the ballast and a more stable track geometry.

The current work aims to provide a methodology to increase the understanding of track settlement in railway turnouts. Different numerical models are used to simulate the dynamic vehicle–track interaction and predict the wheel–rail impact loads in the crossing panel. The calculated contact pressure between sleepers and ballast is used as input for calculating the track settlement. Both empirical and constitutive settlement models are applied to predict settlement for a large number of load cycles (wheel passages). The material behaviour of the track substructure under repeated loading is investigated using a three-dimensional finite element model. A parameter study is performed to determine the influence of train and track parameters on the impact load generated at the crossing. The investigated train parameters include vehicle speed, lateral wheelset position and wheel profile, while the track parameters are rail pad stiffness, sleeper base area and implementation of under sleeper pads (USP). The study shows that the magnitude of the impact load is influenced more by the wheel–rail contact geometry than by the rail pad stiffness. Among the investigated parameter combinations, the most effective mitigation measures to reduce sleeper–ballast contact pressure are the implementation of USP and increasing the sleeper base area.

Keywords: Switches and crossings, turnout, track settlement, vehicle–track dynamics, wheel–rail contact, Green's functions, cyclic loading, material modelling of ballast

To my husband

Anders Fredriksson

Who is my anchor in life and source of stability

and

To my mother

Jiang Yi

Whose passion for learning and working ethics has made me who I am

PREFACE

First of all, I would like to thank my main supervisor Professor Jens Nielsen for guiding me into the world of railway research. Your academic rigour and pedagogical thinking will have a life-long influence on me. If I may, I would like to steal a pinch of your art in academic writing too. I would like to thank my co-supervisors Dr Peter Torstensson, Professor Magnus Ekh and co–author Dr Björn Pålsson for inspiring discussions and enlightening advice. It has been a great experience working with you. Co-supervisor Professor Elena Kabo is specially thanked for her unconditional support during my toughest time. Without you, I would not have made it this far.

I would like to thank all my old friends from the third floor for creating such a pleasant place to work in. Thanks to Kjell Mattiasson for your cheerful company in the past decade. Thanks to Rostyslav Skrypnyk and Emil Aggestam for sharing the journey of the vehicle dynamics conference. It has been great fun. Thanks to all my roommates: Motohide Matsui, Kazuyuki Handa, Nasim Larijani, Lina Wramner and Marko Milosevic. It is a pleasure to have shared office with all of you. Many thanks goes to my manager Peter Folkow, and to Peter Möller, Carina Schmidt, Pernilla Appelgren Johansson as well as Anna-Lena Larsson for making the Dynamics division a family-like place for me to come back to.

I would like to thank the members of the TS15 reference group; Mr Uwe Ossberger and Mr Heinz Ossberger from voestalpine VAE GmbH, Dr Arne Nissen from Trafikverket, Mr Björn Lundwall from Vossloh Nordic Switch Systems AB and Professor Jan Lundberg from JVTC at Luleå University of Technology for their help and valuable input. Mr Ingemar Persson, DEsolver AB, has provided generous support with GENSYS in the beginning of the project. Professor Roger Lundén and Professor Anders Ekberg are greatly appreciated for employing me and for providing the inspirational research environment CHARMEC.

Finally, I would like to thank my family for their support throughout the years. Many thanks to my in-laws Eva and Bosse for helping out whenever we need you. Thank you father for being here when I needed before my dissertation. Thank you mother, for understanding me and supporting me all my life and being my role model. At last, thank you Anders for believing in me and supporting me whatever I decide. You are my strength to come this far. Now, our Fenix and Nova have brought me more power. I must be the luckiest woman on earth to have you all.

ACKNOWLEDGEMENTS

Thesis

This thesis consists of an extended summary and the following appended papers:

Paper A X. Li, J. C. O. Nielsen and B.A. Pålsson. Simulation of track settlement in railway turnouts. *Vehicle System Dynamics* **52** (2014) 421-439. DOI: 10.1080/00423114.2014.904905

Paper B X. Li, M. Ekh and J. C. O. Nielsen. Three-dimensional modelling of differential railway track settlement using a cycle domain constitutive model. *International Journal for Numerical and Analytical Methods in Geomechanics* **40**.12 (2016) 1758-1770. DOI: 10.1002/nag.2515

Paper C X. Li, P. T. Torstensson and J. C. O. Nielsen. Simulation of vertical dynamic vehicle–track interaction in a railway crossing using Green's functions. *Journal of Sound and Vibration* **410**.1 (2017) 318-329. DOI: 10.1016/j.jsv.2017.08.037

Paper D X. Li, J. C. O. Nielsen and P. T. Torstensson. Simulation of wheel–rail impact load and sleeper–ballast contact pressure in railway crossings using a Green's function approach. *Submitted for international publication*

Papers A, B, C and D were prepared in collaboration with the co-authors. The author of this thesis was the main responsible for the major progress of the work, i.e. took part in planning of the papers and the development of the theory, carried out the numerical implementation and simulations, and wrote the papers.

Contents

Part I

Extended Summary

1   Introduction

The railway turnout (switch and crossing, S&C) is a critical component in the railway system [1]. It provides flexibility in traffic routes by allowing the trains to switch from one track to another in a safe and convenient way. To serve this purpose, the turnout typically consists of both movable and fixed mechanical parts, as well as signalling and electrical systems. In Sweden alone, there are about 14 000 S&Cs in the 16 600 km of railway. According to a life cycle cost (LCC) study, based on information from databases at former Banverket (the Swedish Rail Administration) in 2009 [2], turnouts accounted for 50% of the registered inspections and 21% of the operation disturbances. The S&Cs consumed MSEK 530 (about MEUR 53), almost 10% of the total maintenance cost during a single year in 2018, standing for the railway subsystem that caused most train delays in Sweden [3].

A main driver for the high maintenance costs is the need to repair and replace switch rails and crossings as these components are often not sufficiently stable in track geometry and rail profile over time. Dynamic wheel–rail contact forces with high magnitudes, resulting in wheel and rail damage and degradation of track geometry, are often generated in the switch and crossing panels due to the discontinuities in rail profiles along the turnout.

One critical contribution to track geometry degradation is track settlement. It is a phenomenon where the horizontal level of the ballasted track substructure decreases in height over time when subjected to traffic loading. Due to the design of the turnout and the variation in track support conditions, the load transferred to the track bed is not uniform and the resulting differential settlement leads to track irregularities. Poor quality in track geometry induces higher dynamic wheel–rail contact forces and increases the degradation rate resulting in further track settlement, and possibly to increased wear, plastic deformation and rolling contact fatigue of the rails. Thus, it is important to understand how settlement evolves under repeated loading to support product development and maintenance procedures of S&Cs with a more uniform load distribution on the ballast leading to a more stable track geometry.

The work in this thesis is an effort towards an optimisation of the railway crossing design to reduce differential track settlement. It is a continuation of the work performed by Pålsson [4] within the CHARMEC project TS13. To solve this problem, this thesis deals with two main topics: one is the simulation of dynamic vehicle–track interaction in the railway crossing and the other is the prediction of track settlement behaviour of the supporting track substructure. The objective of this work is to develop tools for numerical studies of differential track settlement in railway turnouts. These can be used

for the optimisation of the S&C design and maintenance planning.

In the extended summary, the components of a railway turnout and track substructure are described in Chapters 2 and 3, followed by survey of the mechanisms of track settlement in Chapter 4. The irregularities in track geometry and stiffness associated with track settlement are described in Chapter 5. Measurements of track settlement in railway turnouts as well as nominal track are reviewed in Chapter 6. Chapter 7 and Chapter 8 are devoted to simulation methods for studies of vehicle–turnout interaction and track settlement. Maintenance and mitigation measures for treating track settlement are discussed in Chapter 9. Chapter 10 contains a summary of the appended papers. Finally, conclusions and suggestions for future work are given in Chapter 11.

2   The railway turnout

The objective of a railway turnout is to allow for the diversion of railway traffic from one route to another, providing flexibility to the railway system. There are various kinds of railway turnouts that satisfy the demands of different traffic conditions, see [5]. In this thesis, the simulations have been carried out for the right-hand railway turnout shown in Figure 2.1.

The railway turnout comprises of a switch panel, a closure panel and a crossing panel. The straight line features the through (main) route, while the section that diverts by following a deviating curve is the diverging route. The outer rails of the through and diverging routes are called stock rails. The traffic direction from the switch panel to the crossing panel is called the facing move, while the reverse direction is the trailing move. The front of the turnout is defined as the point where the diverging route starts to deviate from the through route at the left end of the switch panel in Figure 2.1. The traffic direction is altered by controlling the switching machines at the front of the turnout. The closure panel connects the switch and crossing panels. The crossing panel contains the crossing, sometimes referred to as the frog, at which the through and diverging routes intersect. Between the wing rails and the crossing rail, there is a discontinuity in the rail profile, allowing wheel flanges to travel along either path. Commonly, the wing rail and crossing rail are casted into one piece, categorised as a fixed crossing. A photo of a fixed crossing is shown in Figure 2.2.

For heavy-haul and high-speed lines, due to the increased dynamic wheel–rail contact loading, a swingnose crossing (moveable crossing) may be used to eliminate the gap between the wing rail and the crossing rail [4]. Opposite to the crossing, alongside the stock rails of the through and diverging routes, are the check rails. These act as constraints
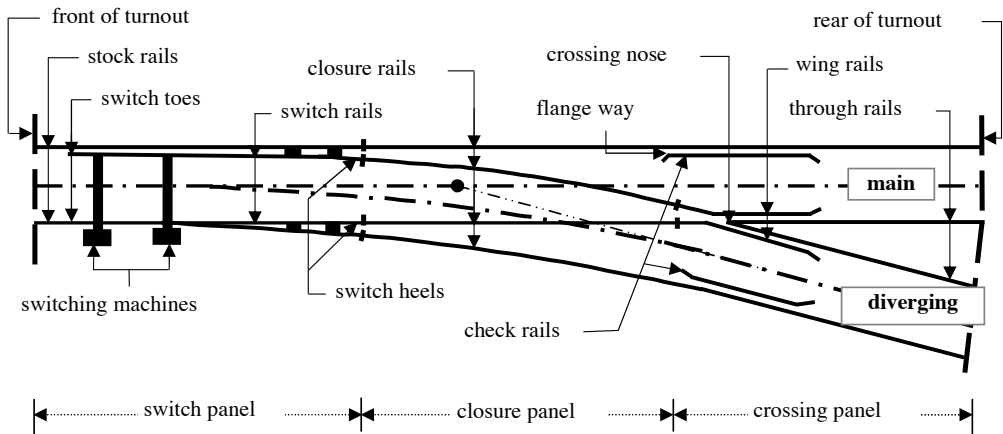
Figure 2.1: *Components of a turnout with main and diverging routes. Dashed lines show the centre lines of the through (main) and diverging routes. From [6]*

for the lateral position of the wheelsets to ensure appropriate flangeway passage and to avoid interference contact between the wheel and the crossing nose [4].

The numerical methods developed in this thesis have been applied for the common Swedish turnout geometry (with a fixed crossing) denoted as 60E1-760-1:15. This means that the turnout has 60E1 rails with curve radius 760 m in the diverging route and a turnout angle of 1:15. The turnout angle is the angle between the centre lines of the through and diverging routes at the crossing, see Figure 2.1.

Figure 2.2: *Overview of crossing panel from the front of the turnout including a fixed crossing and check rails. Photo provided by voestalpine VAE GmbH*

3 Track substructure

A typical railway track on ballast consists of the superstructure and the substructure [7]. The superstructure consists of the rails, the fastening systems and the sleepers (bearers), whereas the substructure consists of the ballast, the sub-ballast and the subgrade [7]. These track components are illustrated in Figure 3.1. Track geotechnology and substructure management are explained in detail by Selig & Waters [7]. The different layers of the substructure will be briefly described in the following.
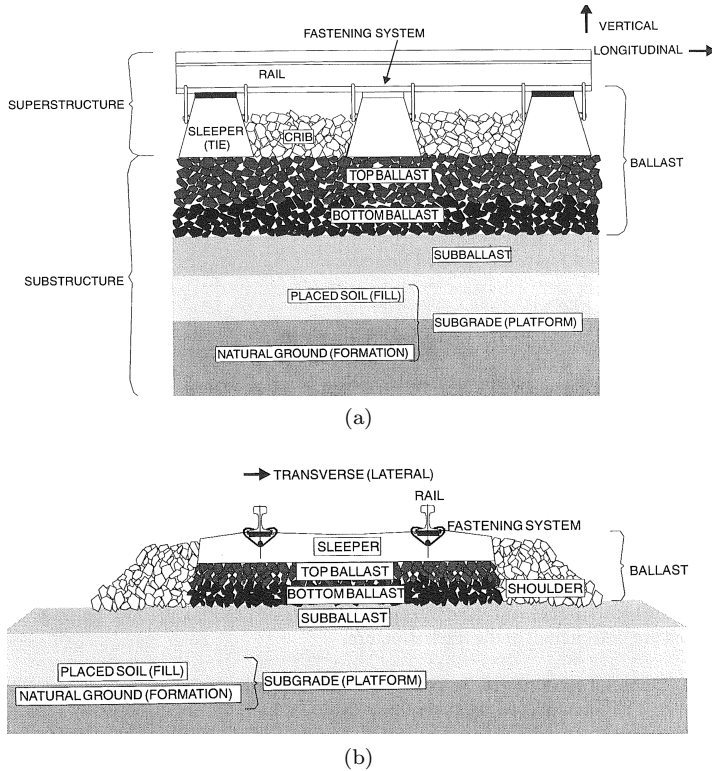
Figure 3.1: *Components of a railway track structure. From [7]*

3.1 Ballast

The ballast is the top-most layer of the track substructure. At the sleeper–ballast interface, the ballast is typically compacted and tamped around the sleepers up to a depth of 0.3 – 0.5 m, see Peplow et al. [8]. According to Raymond [9], the most important features of ballast are:

- Ensure stability of each individual sleeper and the complete track structure
- Provide track resilience, distribute loads from the sleepers to the subgrade, and absorb energy generated by the dynamic wheel–rail contact forces

- Resist variations in weather conditions. Allow for immediate drainage and storage of fouling[1]
- Allow for easy adjustment of track geometry during maintenance

It is difficult to find a granular material satisfying all of these requirements at the same time. For example, increased angularity and roughness of the ballast particles increase the shear strength of the complete track bed and the risk of particle breakage. Further, a balance between bearing capacity and drainage needs to be achieved. High bearing capacity requires that the ballast particles are angular and well-graded[2], but this may lead to poor drainage caused by infiltration and fouling [7]. Typically, coarse-sized, angular-shaped, non-cohesive and uniformly-graded granular material is used to support the track superstructure [8]. Indraratna et al. [11] presented a review of track geotechnology considering the influence of increasing speeds and axle loads.

3.2 Sub-ballast

The sub-ballast is an intermediate granular layer to prevent the intermixing of ballast and subgrade, provide effective drainage and avoid frost penetration. Common suitable sub-ballast materials are broadly-graded natural or crushed sand-gravel mixtures [7]. Geotextile or geosynthetic reinforcements can be applied in this layer to strengthen its capability, see Indraratna et al. [11].

3.3 Subgrade

The subgrade is the platform upon which the track structure is constructed. Its main function is to provide a stable foundation for the sub-ballast and ballast layers. Subgrade conditions can vary over a wide range depending on the geological environment and the conditions at the construction site. The subgrade can for example be soft clay, sand or stiff rock [7]. The soil conditions of the layered subgrade determine the wave speeds of the ground and the fundamental track resonance frequency [12]. A review on the dynamic behaviour and stability of the soil foundation in heavy-haul railway tracks is given by Lazorenko et al. [13]. The soil increases in volume when saturated or frozen, leading to an uplift deformation of the track. Silty soil reduces the bearing capacity. For fine-dispersed soil, progressive shear deformation can occur under repeated traffic loading, where the soil is gradually squeezed out in the direction of lower resistance. Intensive plastic deformation of subgrade can lead to the formation of ballast pockets [14]. Preventive measures, such as adding protective layers (reinforcement layers, water-proofing layers, separating layers, frost protection layers and vibration protection layers), improving the soil quality

---

[1]Fouling is when the gaps between ballast particles are being filled with particles smaller than 6 mm in diameter. Fouling can be caused by various sources: sleeper wear, ballast breakdown, infiltration from the ballast surface or from underlying layers and alleviation due to frost, see Selig & Waters [7].

[2]Ballast gradation determines the particle size distribution. *Well-graded* granular material contains a good representation of all particle sizes from large to small and is characterised by high density, low void content, good interlocking and low permeability. *Poorly-graded* granular material is equal to *uniformly-graded* material in the sense that most of the particles are of about the same size and are characterised by low contact area, poor interlocking, low density and high void content. *Gap-graded*, also called *broadly-graded*, granular material can be either a well-graded or poorly-graded soil lacking one or more intermediate sizes within the range of gradation [10]

(mixing of soils, modification with cement, polymer or limestone) or reinforcing the soil structure (pile reinforcement, prefabricated vertical drain) are discussed extensively by Lazorenko et al. [13]. According to Peplow et al. [8], despite many studies to understand the behaviour of soil in a railway foundation, very little can be done to alter the soil properties during works of maintenance.

4 Mechanisms of track settlement

Models for the prediction of track settlement have been reviewed by Dahlberg [15]. Two major phases in the settlement of ballasted track can be distinguished: (1) the rapid settlement directly after tamping followed by (2) a slower settlement phase. The rapid settlement phase is caused by volume reduction due to rearrangement and consolidation of the granular material. The slower settlement phase can for example be approximated as linear with the number of load cycles (see e.g. Sato [16]), or as logarithmic (see e.g. Alva-Hurtado & Selig [17] and Shenton [18]). The modelling of track settlement is described in Chapter 8.

Dahlberg [15] summarised several mechanisms explaining the ballast and subgrade behaviour in the second (slower) settlement phase:

- Volume reduction caused by particle rearrangement due to repeated train loading
- Volume reduction caused by particle breakdown; i.e. ballast particles may fracture (divided into two or more pieces) due to the loading
- Volume reduction caused by abrasive wear; i.e. originally cornered stones become rounded, thus occupying less space
- Penetration of sub-ballast and/or subgrade into ballast voids
- Inelastic recovery at unloading or stress removal
- Movement of ballast and subgrade particles away from under the sleepers causes the sleepers to sink into the ballast/subgrade

For most tracks, Selig & Waters [7] stated that the degradation of the ballast and sub-ballast layers is the main source of track settlement between maintenance operations. The contributions from different parts of the substructure to the total track settlement under cyclic traffic loading are sketched in Figure 4.1. Necessary conditions for the ballast layer to be the main source of track settlement are: (1) the existence of a separation layer between the coarse ballast and the fine subgrade, (2) a sufficiently strong sub-ballast and subgrade combination, and (3) good drainage of water entering from the surface. In other situations, the track maintenance cycles could instead be dictated by subgrade problems. Subgrade failure can evolve in several ways:

- Excessive progressive settlement and progressive shear failure due to cyclic traffic loading
- Consolidation of settlement and massive shear failure under the combined weights of train, track superstructure, ballast and sub-ballast
- Volume change caused by moisture
- Frost heave and thaw softening

Ballasted track has a property that may lead to that the long-term geometry from before the maintenance is returned (this is sometimes referred to as ballast memory). Figure 4.2 illustrates an example of track geometry before and after tamping [7]. Although the track can be levelled after ballast maintenance, due to the non-uniform initial quality of the individual track components, faults in track geometry may develop at different rates. In [19], it was observed that track geometry after maintenance did not return

to the quality of the track before the previous tamping and that the degradation rate increased with each maintenance intervention. If the track is of good inherent quality, it takes a longer time for the track to deteriorate to the level when the next tamping is required. The results from triaxial tests of granular material have been used to establish an aggregate index to predict deformation and breakdown of ballast under cyclic loading [8].
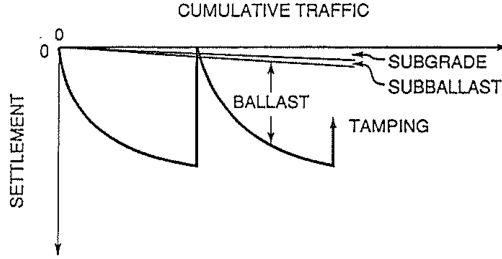

Figure 4.1: *Principle sketch of substructure contributions to track settlement. From [7]*
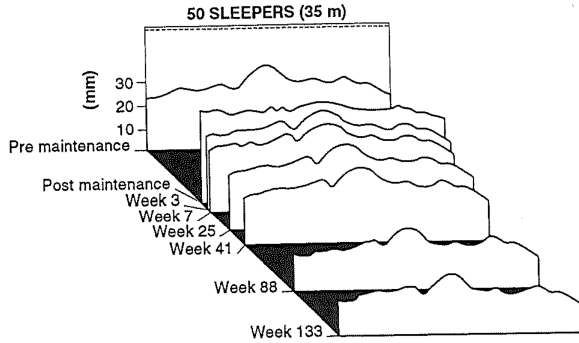

Figure 4.2: *Measured longitudinal level of rail head profile over time, illustrating that track geometry after 133 weeks of traffic has inherited its geometry from the premaintenance geometry (geometry before tamping). From [7]*

5 Irregularities in track geometry and stiffness

Non-uniform track settlement, where the level of settlement varies along the track, leads to irregularities in both track geometry and track stiffness. In this thesis, the non-uniform track settlement is referred to as differential settlement. Irregularities in track geometry are generally classified into four major categories, see Andersson et al. [20]. Longitudinal level is the mean value of the vertical irregularities of the left and right rails, whereas line irregularity is the mean value of the lateral irregularities of the left and right rails. Further, cant irregularity is the deviation from the nominal cant, while gauge irregularity is the deviation from the nominal track gauge, see Figure 5.1.

It is important to characterise and quantify the quality of track[3] after its construction and after maintenance. In this context, the standard deviation of the track irregularity in a given wavelength interval and over a given distance is commonly used as a track quality index[4]. The wavelengths of track geometry irregularities are classified in three intervals according to the European standard EN 13848-5 [21]:

- D1: short wavelength range $3\,\mathrm{m} < \lambda < 25\,\mathrm{m}$
- D2: medium wavelength range $25\,\mathrm{m} < \lambda < 70\,\mathrm{m}$
- D3: long wavelength range $70\,\mathrm{m} < \lambda < 150\,\mathrm{m}$ for longitudinal level and $70\,\mathrm{m} < \lambda < 200\,\mathrm{m}$ for line irregularity
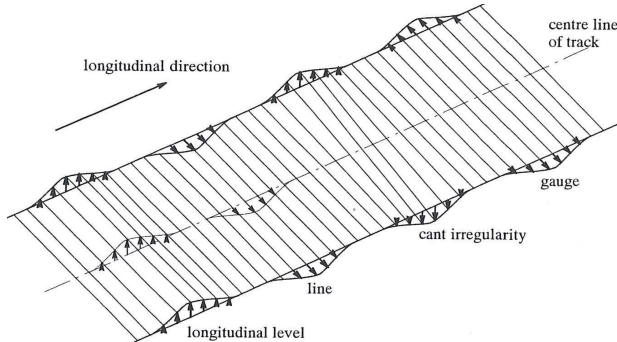
Figure 5.1: *Definition of track irregularities: longitudinal level, line, cant irregularity and gauge. From [20]*

---

[3]Track geometry quality is one of the main factors that relates to maintenance planning. It is defined in EN 13848-5 [21] as an assessment of the deviation from the mean or designed geometrical characteristics of specified parameters in the vertical and lateral track planes, which give rise to safety concerns and/or have a correlation with ride quality.

[4]Track quality index (TQI) is the value that characterises track geometry quality of a track section based on parameters and measuring methods compliant with the EN 13848 series. Indices used to assess track quality, described in EN 13848-6 [22], are based on: (1) extreme values of isolated geometry defects represented by the deviation from the mean value to the peak value, or from zero to the peak value; (2) standard deviation over a defined length (typically 200 m and in a given wavelength range), representing the variation of a signal over a given track section in relation to the mean value of this signal over the considered section; (3) mean value.

If the level of compaction is not uniform, or if the material properties of the track substructure vary along the track, there will be an initial differential settlement directly after construction or tamping leading to irregularities in track geometry. These irregularities in geometry (and stiffness) induce a dynamic loading under repeated train traffic that may result in further differential settlement. According to Fröhling [23], in the low-frequency range, the spatially varying track settlement contributes significantly to irregularities in longitudinal level and cant.

Differential track settlement typically leads to a consolidated track substructure and a spatially varying track stiffness. The vertical stiffness of a railway track is determined by the combined resilience of rails, rail pads, sleepers, under-sleeper pads (USP), ballast, subballast and subgrade [24]. The variation in stiffness along the track will induce dynamic wheel–rail contact forces and vibrations. The rate of degradation of track components and the rate of track settlement will depend on the severity of the stiffness variation [25]. The influence of vertical track stiffness variation on track settlement has been investigated by Fröhling [23]. A guide for track stiffness including measurement techniques, modelling methods, problems caused by track stiffness variation in different sections of railway track and their potential remedies have been summarised by Powrie & Le Pen [26].

Locations that are particularly prone to high track stiffness variations are rail joints, transition zones and S&Cs:

Rail joint At a rail joint, the loading of the gap between the two rails jointed by fish plates typically results in a dipped joint that induces dynamic loads leading to rail degradation and track settlement. The joint leads to a sudden variation in dynamic track stiffness because of the change in bending and shear stiffnesses over the jointed rail and the added weight from the fish plates [27].

Transition zone The vertical track stiffness may change at transitions in the track substucture, such as at the transition from a ballasted track to a bridge or from a slab track to a ballasted track. This often leads to problems with differential track settlement on the ballasted track side, see Li & Davis [28], Coelho et al. [29] and Wang et al. [30].

S&C S&Cs contain several irregularities both in terms of geometry and stiffness. In the switch panel, there is a variation in rail geometry to allow for the wheels to transfer from the stock rail to the switch rail. In the crossing panel, a discontinuity exists in the rail profile between wing rail and nose rail. Besides the kinematic aspects of turnout irregularities, the variation in turnout stiffness is significant. The sleepers (bearers) have different lengths and different spacings. The track stiffness at the left and right rails is different due to the asymmetry of the turnout design. The variation in rail profiles in the switch and crossing panels leads to variations in rail bending stiffness and mass. These abrupt changes in track geometry, stiffness and mass can lead to the excitation of transient and high-frequency vibrations in the train–track dynamic system.

When differential track settlement evolves, the phenomenon of voided sleepers (hanging sleepers) may occur. This means that the sleeper is partially supported or not supported by the ballast. The track stiffness at voided sleepers is lower than at the adjacent supported sleepers. Each passing wheel may generate an impact load between the sleeper and the ballast (if sleeper–ballast contact occurs due to the wheel load) and further track degradation, see Augustin & Gudehus [31], Bezin et al. [32], Zhang et al. [33] and Nielsen & Li [34].

6 Field and laboratory measurements

The first part of this section is dedicated to the measurements of track irregularity, track settlement and track stiffness. The second part is on the measurement of properties of granular materials.

6.1 Track irregularity and track stiffness

To measure track irregularity and track stiffness, field measurements (also called *in-situ* tests) are commonly used. Berggren [35] categorised the measuring techniques into *standstill* measurements and *rolling* measurements.

6.1.1 Standstill measurements

In *standstill* measurements, sleepers and/or rails are instrumented with displacement transducers or accelerometers and the response during the passage of a train is measured. The sensor types include lasers, multidepth deflectometers, accelerometers, high-speed film cameras with digital image correlation (DIC), velocity transducers (geophones), etc. A review of available technologies and methods is given by Powrie & Le Pen [26]. Some important measurement results are summarised below.

Fröhling [23] used an instrumented test train to measure the degradation of track stiffness and track geometry on a track section of a heavy-haul line in South Africa. Multidepth deflectometers were used to determine the stiffness of different substructure layers. A high correlation between spatially varying track stiffness and differential track settlement was found. A motivation for the work in the current thesis is to develop simulation methods that account for the spatially varying track stiffness (in longitudinal and lateral directions) of a railway turnout.

In the EU project TURNOUTS [36], measurements were conducted on different types of urban turnouts to evaluate various designs to reduce wheel–rail impact forces, such as a geometry modification of the gauge corner in the switch panel and the implementation of a swingnose crossing. Improved ride comfort and reduced maintenance needs were reported. The study also found a low sensitivity to different wheel profiles or worn wheels when using the swingnose crossing. The measured results were used to calibrate two models for simulation of dynamic vehicle–track interaction and ground vibration, respectively, see Bruni et al. [37].

Wan et al. [38] investigated the effect of crossing geometry on the dynamic behaviour of a turnout. It was observed that poor crossing geometry before grinding resulted in a higher maximum vertical acceleration of the crossing nose. The lateral acceleration was lower in magnitude than the vertical acceleration and less sensitive to the variation in crossing geometry.

Paixão et al. [39] carried out field measurements to investigate the effect of USPs at a transition zone onto a bridge. The results indicated that the USPs influence the dynamic behaviour of the track, increasing its vertical flexibility and amplifying both rail displacements and sleeper accelerations.

Wang et al. [30] used a DIC device to measure rail vertical displacements at multiple points in a transition zone. The study provided methods for long-term monitoring and quality assessment of differential settlement in transition zones.

Le Pen et al. [40] also used a DIC device to monitor the vertical displacement of sleepers at a level crossing, where unsupported and hanging sleepers were identified on locations close to the crossing. Further, the influence of implementing soft or medium stiffness USPs in a turnout was measured in [41]. As expected, the measurements also showed that for elongated sleepers, soft USPs led to larger sleeper vertical displacements and sleeper bending. The displacements can be reduced by casting or gluing a modified roughened facing on the side of the USP towards the bottom of the sleeper.

In the *standstill* measurements reported by Jönsson et al. [42], the unloaded vertical track geometry of 1:15 and 1:14 turnouts on ballast relative to a fixed reference point was monitored. The influence of climate conditions and the choice of reference point for *standstill* measurements on the quantatitive results of differential settlement at the railway crossing was discussed.

In the work of Oscarsson [43], field measurements of sleeper support stiffness and dynamic behaviour of railway track were performed at two test sites in Sweden. A large scatter in the support stiffness of ballast/subgrade was observed. Similar results were reported by Le Pen et al. [44], where the track support stiffness at 209 adjacent sleepers of a high-speed ballasted track was measured.

6.1.2 Rolling measurements

In *rolling* measurements, the track stiffness is measured with a track recording car continuously along the track [35]. In Sweden, the Rolling Stiffness Measurement Vehicle (RSMV) was designed to measure the dynamic track stiffness for frequencies up to 50 Hz [35]. The RSMV is a rebuilt two-axle freight wagon that excites the track using two oscillating masses above one of the ordinary wheel axles. Track stiffness is determined based on the measured force and acceleration, see Figure 6.1. Alternatively, track stiffness can be measured using a track geometry recording car STRIX/IMV100/IMV200 [19, 45], extended with sensors to measure rail vertical displacement at different distances from the wheels. This system allows for measurement of longitudinal level in both loaded and unloaded conditions to determine the track stiffness. Studies that utilised the above methods for measuring track geometry and dynamic track stiffness at S&Cs and on the heavy-haul line in Sweden are listed below.

In Kassa & Nielsen [46], the RSMV was used to measure the vertical dynamic track stiffness along a turnout. Further, lateral and vertical wheel–rail contact forces were measured using a wheelset instrumented with strain gauges mounted on the wheel discs. The influences of train speed, traffic direction and route on the magnitude and position of the maximum lateral contact force in the diverging route of the switch panel, as well as on the maximum vertical contact force in the crossing panel, were investigated. The measured contact forces were compared with simulations. Both measurements and numerical simulations showed an increase in the maximum lateral contact force with increasing train speed in both the facing and trailing moves. The travelling route (main

or diverging) was found to have a large influence on the maximum vertical contact force at the crossing.

In Pålsson & Nielsen [47], measurement data from RSMV was used to calibrate the track models of two Swedish turnouts with an implementation of soft or stiff rail pads. The measurements were performed for traffic in both the through and diverging routes, and in the facing and trailing moves. The study found that impact loads on the crossing can be reduced by using more resilient rail pads. In the EU project INNOTRACK [48, 49], the dynamic track stiffness was also measured with this method.

In Bolmsvik et al. [50], field measurements of wheel–rail contact forces and sleeper bending moment were evaluated for two 60E1-760-1:15 turnouts at Härad and Eslöv, Sweden. The turnout in Eslöv featured softer rail pads (stiffness of 120 kN/mm) compared to the stiffer configuration in Härad (a factor of ten times stiffer). In parallel, the RSMV was used to measure the track stiffness per rail along the turnout. A finite element model of the complete turnout was validated in [50] by comparing calculated and measured sleeper bending moments. In **Paper A** and **Paper B**, the track model is based on the Härad data, while in **Paper C** and **Paper D**, the model is based on the conditions at the Eslöv turnout.

In Nielsen et al. [19], the data measured by STRIX/IMV100 was used to analyse the track stiffness on a section of the Swedish heavy-haul line and the track geometry degradation from 1999 to 2016. A correlation between measured track stiffness gradient and differential settlement was reported. It was shown that recurrent severe local track geometry irregularities often occur on track sections where there is a combination of a low magnitude and a high gradient in the substructure stiffness. Measures such as upgrading of the ballast and subgrade layers were recommended as a more cost-efficient option to improve track geometry in the long-term.

In Khouy et al. [51], the longitudinal level of a turnout on the Swedish heavy-haul line
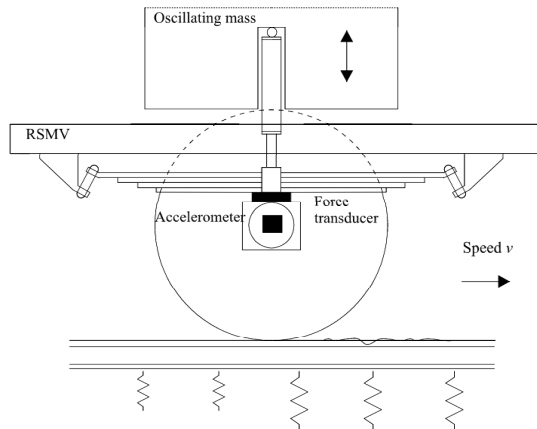

Figure 6.1: *Measurement principle of RSMV. From [35]*

was measured at predefined time intervals using the STRIX/IMV100 track measurement car. The proposed measurement method was used to determine the growth rate of the longitudinal level degradation as a function of million gross tonnes (time).

6.2 Properties of granular material

Depending on the dimensions of the test sample, laboratory tests on granular material can be sorted into simple triaxial tests and full-scale tests.

6.2.1 Triaxial tests

In a triaxial test, the test sample only includes a small section or part of the track substructure (ballast, sub-ballast and subgrade). The sample is processed and put into a triaxial test container, subjected to a confining pressure. A vertical load with controlled magnitude and frequency is applied at the top of the specimen. The size of a triaxial test is decided by the representative volume of the material sample.

Early experimental studies with a repeated load on a granular material were performed by Raymond & Williams [52]. The results were used to generate an aggregate index to predict deformation and breakage. Triaxial tests by Suiker & Selig [53] were used to study the static and dynamic responses of ballast material. It was found that under cyclic loading, the granular materials reveal a strong tendency to compact, even if the applied stress level is close to the static failure strength of the material. This compaction behaviour generally causes a significant increase of the material stiffness. Indraratna et al. [54] used data from a large triaxial test to establish a nonlinear relationship between the shear strength, the angle of internal friction, dilatation rate and degree of particle crushing at different levels of confining pressure and principle stress ratios.

Settlement influenced by particle breakage and confining pressure was studied in Lackenby et al. [55]. It was found that there exists an optimum range of confining pressure for each considered deviatoric stress. A low confining pressure can lead to excessive axial deformation and particle breakage. For tracks subjected to high axle loads, the lateral pressure should be increased to prevent excess settlement. Indraratna et al. [56] investigated the influence of ballast fouling. The study suggested that fouled ballast has less particle breakage due to increased particle contact area and reduced maximum contact pressure. In some studies, the results of triaxial tests have been used to calibrate material models of ballast or to validate discrete element models, see e.g. Li & McDowell [57]. Image analysis techniques have been used to measure the three-dimensional stress field of granular material during loading and unloading, cf. Dijkstra et al. [58, 59].

Many triaxial tests have shown that there are indications of the existence of a threshold stress ratio, below which the permanent strain does not grow, and beyond which the material experiences incremental collapse or gradual failure, see Lekarp [60], Werkmeister et al. [61], Garcia-Rojo & Herrmann [62]. The threshold stress ratio is related to the shakedown limit, a concept that is used in the material model implemented in **Paper B**. Sun et al. [63] investigated the influence of train speed (represented by the frequency of the applied loading) using a large-scale triaxial test. It was found that the shakedown characteristics of granular materials were dependent on the frequency of the loading.

For track on high-speed lines, an increasing confining pressure helped to prevent ballast breakdown.

6.2.2   Full-scale tests

Full-scale laboratory tests require a test rig with such dimensions that a track section corresponding to several sleeper bays can be accommodated. The test rig is often capable of accommodating one or multiple sleeper segments and adjusting the depth of the substructure.

Baessler & Ruecker [64] used a geotechnical test rig to study the influence of the minimum magnitude load during cyclic loading on track settlement. The study showed that the ballast layer is subjected to increased settlement at the presence of a threshold vertical load level during unloading. This implies that high dynamic loading such as above voided sleepers or due to track irregularities, can lead to a higher rate of track settlement.

Abadi et al. [65] carried out cyclic loading tests in the Southampton Railway Testing Facility. The test consisted of a laboratory apparatus representing a single sleeper bay under plain strain conditions. Various designs, such as improving the ballast grading, reducing the ballast shoulder slope, the adoption of different sleeper types and modifications to the sleeper/ballast interface, were investigated. It was concluded that the use of finer ballast gradings and a shallower shoulder slope has the potential to reduce maintenance requirements.

In **Paper B**, measurement data from a laboratory test at CEDEX in Spain [66] is used to calibrate and verify a cycle-domain constitutive model of a granular material. The rail track accelerated testing facility at CEDEX includes a 21 m long, 5 m wide and 4 m deep box to accommodate the track substructure. Complete railway actuator cylinders, separated 1.5 m from each other, are deployed to apply loads on the rails over seven consecutive sleepers. For the long-lasting test, track substructure status has been examined corresponding to 200 000 freight axle passages per day.

Figure 6.2: *Assembly of geotechnical test rig at CEDEX. From [66]*

7 Simulation of dynamic vehicle–turnout interaction

The first step in a numerical prediction of differential track settlement is to simulate the dynamic vehicle–track interaction, as the cyclic loading of the track system is the main cause to track settlement.

In this chapter, the general principles of the dynamic excitation by the wheel load is illustrated, followed by a description of the wheel–rail kinematics in the crossing panel. Then the different parts of the simulation methodology applied in this thesis are explained in the following order: time integration methods, track model, wheelset model and wheel–rail contact models.

7.1 Wheel load excitation

The wheel loads applied on the track by the moving rail vehicles are composed of a static load and a dynamic component superimposed on the static load. The deformation of the rail and the load distribution in the track due to a static wheel–rail contact force is sketched in Figure 7.1. It is commonly assumed [7] that the sleeper directly below the wheel–rail contact supports around 50% of the wheel load, while the two adjacent sleepers on each side of the wheel support around 25% each (the true fractions of the load are dependent on track properties, such as the type of rail and the stiffness of rail pads and ballast/subgrade). Further away from the wheel load, a small uplift of the rail may exist due to rail bending. If the uplifting force is not compensated for by the weight of the track superstructure and by frictional forces from the ballast applied on the sides of the sleeper, one or a few sleepers may lift momentarily. The longitudinal motion of the wheel will lead to a cyclic loading of the track. The track deterioration is influenced by the magnitudes of the dynamic wheel–rail contact forces induced by wheel/track irregularities and the vehicle–track interaction [67]. The traffic-induced stresses in the substructure can transfer as deep down as five metres below the bottom surface of the sleepers [7]. Some studies on the influence of the vehicle loading on track settlement are shortly reviewed below.

According to Iwnicki et al. [68], tracks carrying fast and heavy trains require more frequent maintenance. Stichel [69] estimated that freight traffic causes $90-95\%$ of the total track deterioration on Swedish main lines. A review on dynamic behaviour and stability of soil foundation in heavy-haul railway tracks was presented by Lazorenko et al. [13]. The review concluded that the track degradation process accelerates under high axial loads.

Ishida & Suzuki [70] studied the effects of train speed, unsprung mass, and the distance between the leading and trailing axles of a bogie on track settlement. It was suggested that if the distance between the axles is less than 4 m, the interaction between the axles must be taken into consideration. The interacting effect of the axles increases with increasing speed, but the unsprung mass has little influence on the interaction between

the axles. This effect is also observed in **Paper A**, where between the passages of the leading and trailing wheelsets of each bogie, the sleeper–ballast contact pressure does not recover to zero as it does between the trailing axle of the leading bogie and the leading axle of the trailing bogie. The influence of train speed, braking/acceleration and heavy axle load on stresses in the track substructure has been investigated by Yang et al. [71]. It was shown that train acceleration/braking may increase shear stresses and horizontal displacements in the soil. With the presence of unsupported sleepers, the soil stress below the adjacent sleepers tend to increase in the ballast and sub-ballast layers, but becomes insignificant with increasing depth.

High dynamic wheel–rail impact loads can also be generated by wheel out-of-roundness. This problem has been addressed by Bezin et al. [72] and Nielsen & Johansson [73, 74].
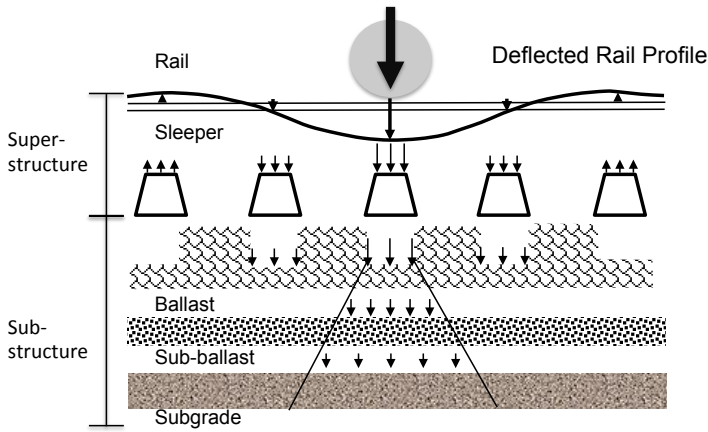
Figure 7.1: *Schematic wheel load distribtuion in the track structure under a static wheel load. From [7]*

7.2   Kinematics in the crossing panel

A wheel passing over the crossing in the facing move (from the switch panel towards the crossing panel) will first make contact with the wing rail. The wheel–rail contact then moves towards the field side of the wheel profile. For a typical conical wheel profile, the rolling radius decreases and the wheel moves downwards unless the wing rail is elevated. When the wheel reaches and makes contact with the vertically inclined crossing nose, the contact load is transferred from the wing rail to the crossing nose. The rolling radius will then increase as the new contact point is closer to the wheel flange, see Figure 7.2. The dynamic vehicle–track interaction typically results in an impact load on the crossing nose as the downward motion of the vertical wheel trajectory is reversed and the wheel is accelerated upwards by the vertically inclined crossing nose.
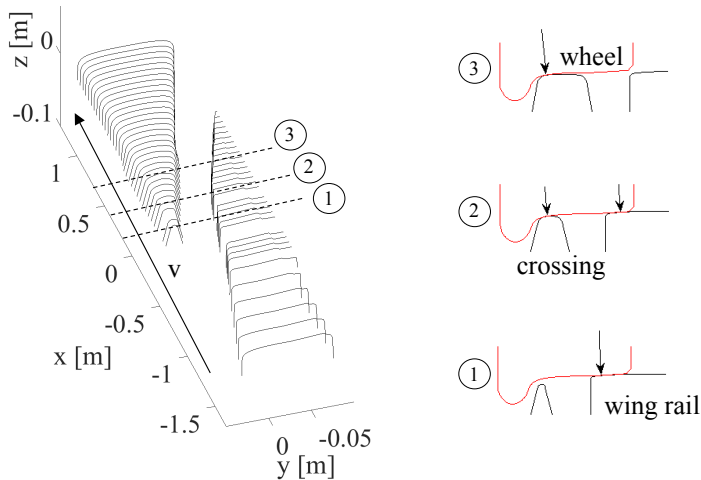
Figure 7.2: *Rail configuration at a crossing illustrating parts of one wing rail and one crossing nose. The crossing transition takes place close to the theoretical crossing point (TCP) of the turnout. From [4]*

7.3 Time integration methods

Models for simulation of dynamic vehicle–track interaction are reviewed by Knothe & Grassie [75] and by Popp et al. [76]. Generally, these are divided into frequency-domain and time-domain models. Frequency-domain models are restricted to linear systems and steady-state harmonic excitation. The vehicle and track responses are assumed to be stationary, implying that transient or singular events such as caused by rail discontinuities, voided sleepers or variation in track stiffness cannot be treated [75]. Time-domain models, on the other hand, can account for different non-linearities in the vehicle–track system but at a higher cost in computation time. This section is dedicated to different approaches of modelling the vehicle–track interaction in the time domain. Special focus is drawn to a methodology based on the use of impulse response functions (Green's functions) to describe the dynamics of wheelset and track. This methodology is used in **Paper C** and **Paper D**.

7.3.1 Finite element model

One way to compute the vehicle–track interaction in the time domain is to use finite element analysis to solve the transient problem. Two main classes of integration schemes exist, namely *explicit* and *implicit* methods [77]. In an *implicit* scheme, the state of a given time step is dependent on quantities from previous time steps and the current time step. Backward Euler time integration is commonly used to discretize the equations of motion [77]. The implicit scheme is unconditionally stable, thus allowing for large time steps. For nonlinear contact problems, the solution generally has to be solved iteratively to satisfy all the contact conditions and the force/moment equilibrium. In commercial software such as ABAQUS [78], if convergence cannot be reached within a reasonable number of

iterations, the time increment is decreased and further attempts are made. For a case with a three-dimensional model with nonlinear material and a large number of possible contact points in changing contact conditions (rolling contact), the implicit method may result in extremely small time increments and convergence difficulties. The implicit method has been used in **Paper B**, where a cycle-domain viscoplastic constitutive model for the track substructure is applied and explored for three-dimensional continuum modelling of ballast settlement with the objective to account for longitudinal variations in load, structure and material properties.

The explicit methods, on the other hand, solve the second time-derivative of the unknown displacements by considering the mass matrix as a 'lumped' diagonal matrix. The forward Euler discretization scheme is commonly used in which the state of the system at a given time increment is computed from the state of the system at the previous time increment [77]. The necessary time increment is independent of the number of contact points and the complexity of the contact conditions. Due to this reason, the calculation of each increment using the explicit scheme is relatively inexpensive compared with using an implicit increment on a similar size model. For rolling contact and dynamic vehicle–track interaction problems where the high-frequency dynamics is important, the explicit method is the preferred alternative. However, the explicit method is only conditionally stable and small time steps are required [79]. To calculate the wheel–rail contact stress in the contact patch, the circumference of the wheel and a section of the rail must be discretized by a dense mesh, resulting in a high computational cost for a long distance simulation of wheel–rail contact [79].

7.3.2 Green's functions

In an integration scheme based on the concept of Green's functions, the vehicle and track are modelled as separate subsystems that interact through the wheel–rail contact forces.

The dynamic response of a linear system subjected to general excitation can be solved using the convolution integral method. The theory of the convolution integral is provided in the book for foundamentals of structural dynamics by Craig & Kurdila [80]. An illustration of the method was given by Andersson [79]. The illustrated example of a suspended mass oscillating due to a unit impulse acting over a short time is repeated here. Consider a one-DOF system with a mass m connected to a linear spring k and subjected to an impulse load $F(t)$ in time period t_d. If the system is initially at rest, the equation of motion can be written as:

$$m\ddot{u} + ku = \begin{cases} F(t) & 0 \leq t \leq t_d \\ 0 & t > t_d \end{cases} \tag{7.1}$$

$$u(0) = \dot{u}(0) = 0 \tag{7.2}$$

where u is the unknown displacement, $\dot{u}$ and $\ddot{u}$ are the first and second time derivatives. Integrating Equation 7.1 over the time interval $[0, t_d]$ yields

$$m\dot{u}(t_d) + ku_\mathrm{avg}t_d = \int_0^{t_d} F(t)\mathrm{d}t, \qquad 0 \leq t \leq t_d \tag{7.3}$$

where u_{avg} is the average displacement. When t_d is infinitely small ($t_d \to 0, t_d = 0^+$), Equation 7.3 becomes

$$m\dot{u}(0^+) = I \tag{7.4}$$

where $I = \int_0^{t_d} F(t)\mathrm{d}t$. Thus, the initial conditions for time interval $t > t_d$ are derived as

$$\dot{u}(0^+) = \frac{I}{m} \tag{7.5}$$

$$u(0^+) = 0 \tag{7.6}$$

The solution to Equations 7.1 to 7.5 yields

$$u(t) = \frac{I}{m\omega_n}\sin(\omega_n t) \tag{7.7}$$

where $\omega_n = \sqrt{k/m}$ is the natural angular frequency.

By setting $I = 1$, the unit impulse response function, also called the Green's function, denoted as $G(t)$ is obtained as

$$G(t) = \frac{1}{m\omega_n}\sin(\omega_n t) \tag{7.8}$$

When the mass is subjected to an entire load history, the total displacement response at an arbitrary time point t is obtained as a superposition of all impulse responses from the previous time steps.

$$\mathrm{d}I = F(\tau)\mathrm{d}\tau \tag{7.9}$$

$$\mathrm{d}u(t) = G(t - \tau)\mathrm{d}I \tag{7.10}$$

$$u(t) = \int_0^t F(\tau)G(t - \tau)\mathrm{d}\tau \tag{7.11}$$

For the track, to account for the motion of the wheel loads, the moving Green's functions are derived by a systematic sampling from a set of inverse Fourier transforms that are based on complex-valued frequency response functions or FRFs (denoted as $g(f)$, where f stands for frequency), see Pieringer [81] for a detailed explanation. The frequency response functions describe the response in one point of the dynamic system when subjected to a harmonic excitation in the same position (direct receptance) or at another position (cross receptances).

For the track model in **Paper C** and **Paper D**, a so-called moving Green's function methodology is applied to account for the motion of the vehicle model along the track. This approach has previously been utilised for simulation of vehicle–track dynamics under the excitation by discrete rail supports [82], rail irregularities [83] and unstable vibrations of the vehicle [84, 85], and for the prediction of squeal noise [81, 86] and rolling contact fatigue damage [79] on standard track. Further it has been used in [87] for the prediction

of impact noise at railway crossings. A detailed explanation of the moving Green's function and how it is assembled can be found in Pieringer [81]. The scheme is briefly illustrated below.

Considering the discretely supported track model in Figure 7.3 and a constant vehicle speed v, the points α, β, δ and γ etc. correspond to the longitudinal positions of $x_n = x_0 + vn\Delta t$, where $n = 0, 1, 2, 3, \cdots N_g$ is the number of sampling points. The ordinary Green's functions $G^{x_0,x_n}(t)$ are obtained from the point and cross receptances $g^{x_0,x_n}(f)$ via their inverse Fourier transforms

$$G^{x_0,x_n}(t) = \mathscr{F}^{-1}(\underline{g}^{x_0,x_n}(f)) \tag{7.12}$$

The moving Green's function $G_v(x_0, t)$ is a superposition of samples from the series of ordinary Green's functions calculated from the points that represent a load moving at train speed v away from the excitation. The total number of sampling points N_g should satisfy that at $N_g\Delta t$, the Green's functions at x_0 of the structure have decayed to almost zero.

According to Equation 7.11, the rail displacement beneath the wheel can be expressed as

$$\xi_R(t) = \int_0^t Q(\tau)G_v(v\tau, t - \tau)d\tau \tag{7.13}$$

Note that the dynamic response is considered at the wheel's current position, as the
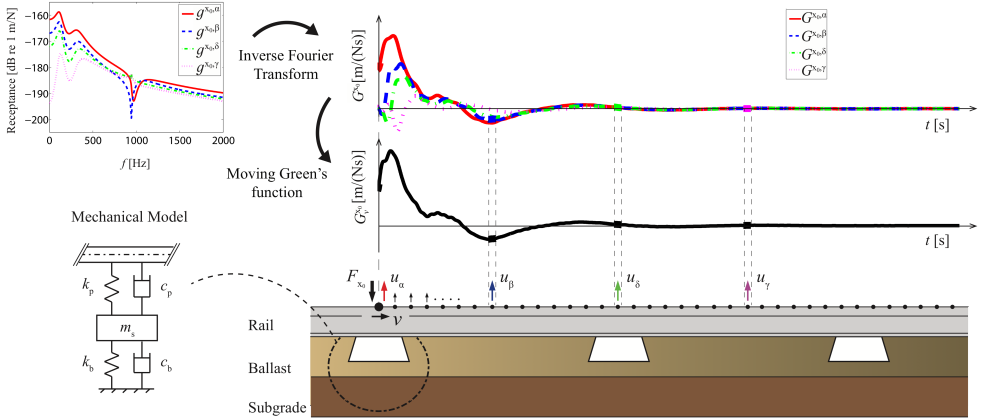
Figure 7.3: *Schematic illustration of assembly of Green's function. Sleeper mass m_s, rail pad stiffness and damping k_p, c_p and ballast stiffness and damping k_b, c_b. Vehicle speed v, time discretisation Δt. Points $\alpha, \beta, \delta, \gamma$ correspond to longitudinal positions $x_\alpha = x_0 + 0v\Delta t$, $x_\beta = x_0 + 1v\Delta t$, $x_\delta = x_0 + 2v\Delta t$, and $x_\gamma = x_0 + 3v\Delta t$. $g^{x_0,\alpha}, g^{x_0,\beta}, g^{x_0,\delta}$, and $g^{x_0,\gamma}$ stand for point and cross receptances. $G^{x_0,\alpha}, G^{x_0,\beta}, G^{x_0,\delta}$, and $G^{x_0,\gamma}$ stand for ordinary Green's functions. Figure generated by Peter Torstensson*

displacement of the rail beneath the wheel is typically of primary interest. The time discretisation in **Paper C** and **Paper D** is determined by the mesh size in the potential wheel–rail contact area and the vehicle speed. For a periodic track model, such as a nominal track, one separate Green's function needs to be calculated for each excitation position within one sleeper bay. For a non-periodic track model, such as one representing a railway crossing, one separate Green's function needs to be calculated for each excitation position along the complete crossing. The work flow for the simulations in **Paper C** and **Paper D** is shown in Figure 7.4.

The procedure of modal decomposition can be used to save computational cost in the calculation of receptances. To account for the non-proportional distribution of damping, a complex-valued modal synthesis method is required to decouple the equations of motion, see Abrahamsson [88] and Nielsen [89]. This method was employed in **Paper C** for the track model of the crossing panel and in **Paper D** also for the flexible wheelset.

Wheel and track models represented by Green's functions can be applied in combina-
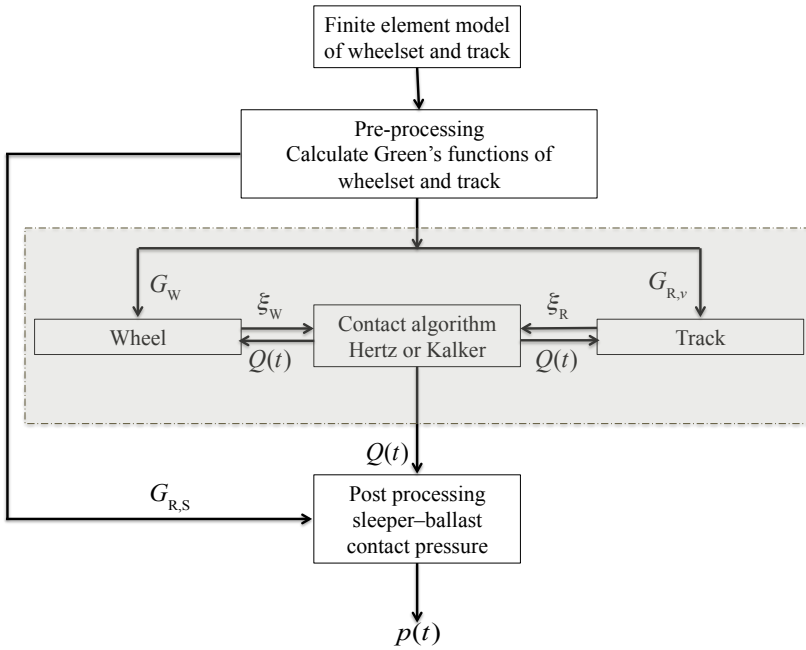
Figure 7.4: *Flow chart describing the in-house vehicle–track interaction software. G_W denotes the Green's functions of the wheelset, $G_{R,v}$ the moving Green's functions of the track and $G_{R,S}$ the Green's functions between the rail and the sleeper. At a given time t, ξ_R and ξ_W denote displacements of the rail and the wheel, Q the wheel–rail contact force and p the sleeper–ballast contact pressure. The dynamic vehicle–track interaction is solved online inside the grey box. The Green's functions of the wheel, the rails and the sleepers are solved in a preprocessor. The sleeper–ballast contact pressure is calculated in a post processing step*

tion with different models of the wheel–rail contact (such as Hertzian contact of Kalker's variational method) without changing the formulation of the interaction model, see [81]. The model can be used to account for the high-frequency dynamics of the wheelset and the corssing panel. However, in this application, any nonlinearity in the vehicle–track system is isolated to the wheel–rail contact. In each time step of the contact detection algorithm, the lateral position of the wheelset centre is prescribed, but the contact positions on the wheel and rail profile are not, allowing for an accurate prediction of the wheel transition between wing rail and crossing nose. This is a reasonable assumption when only the vertical dynamics is of interest, as is the case for track settlement in a railway crossing. Since the method is restricted to linear systems, nonlinearities in the track model such as unsupported sleepers or non-linear track substructure properties cannot be incorporated in the Green's function representation.

7.4 Track models

In a simulation of dynamic vehicle–track interaction, the level of detail required for the track model is determined by the frequency range of interest [90]. In the survey [75, 76], several highly-damped resonances in the track system are discussed. Some of the major comments are summarised below.

For a layered track structure on top of a subgrade which is less stiff than the ballast and sub-ballast, a track resonance may appear in the frequency range 20 – 40 Hz. In this frequency range, the resonance is mainly determined by the soil conditions. In order to capture this resonance in a track model, the inertia (mass) of the subgrade needs to be accounted for. This resonance may be called embankment vibration. This subject has been investigated by Oscarsson [43].

In the frequency range 50 – 300 Hz, there is another track resonance where the track superstructure (rail and sleeper) is vibrating on the ballast and the subgrade support. The rails and sleepers are vibrating in phase on the support stiffness.

In the frequency range 200 – 600 Hz, there is a rail on rail pad vibration where the rails and sleepers are vibrating out of phase. Each rail pad acts as a spring and damper inserted between rail and sleeper. The ballast supplies most of the damping. Another significant track resonance (but with low damping) is the so-called pinned-pinned resonance (for a nominal rail at around 1000 Hz), where the vibration wavelength of the rail is equal to twice the distance of the sleeper spacing. In this case, the track substructure absorbs little energy from the excitation.

When the non-linear characteristics of the track structure are taken into account (in particular, the properties of rail pads, ballast and subgrade are non-linear), the properties of the track are not only a function of frequency but also of the amplitude of the load excitation [91].

7.4.1 Moving track model

A so-called moving track model is represented by a co-following mass-spring-damper system that is coupled to each wheelset in the vehicle model. A common type of moving track model used in several software for simulation of low-frequency vehicle dynamics (e.g. GENSYS [92]) consists of two rails with neglected inertia that are attached to one track mass by spring-damper elements in the lateral and vertical directions to account for the dynamic stiffness of rails and rail pads. The remaining track flexibility is represented by spring-damper elements that connect the track mass to a rigid ground. Some studies where a moving track model has been used for simulation of vehicle–turnout interaction are reviewed below.

Kassa & Nielsen [46] studied the applicability of the moving track model (GENSYS) for low-frequency train–turnout interaction by comparing the results with measured lateral and vertical wheel-rail contact forces. It was concluded that the GENSYS model is useful for the prediction of lateral contact forces in the switch panel, as a three-dimensional model of the vehicle–track interaction can be included and simulation times

are short.

In Pålsson & Nielsen [47], two moving track models with or without the modelling of ballast mass and stiffness were compared and validated versus field measurements, and the influence of rail pad stiffness was studied. By including the ballast mass, the moving track model could be tuned to capture the phase delay in dynamic track stiffness at low frequencies, which has been observed in the data from a track stiffness measurement vehicle. It was also concluded that impact loads on the crossing can be reduced by using more resilient rail pads.

Wan et al. [93] calibrated a moving track model by comparing the calculated vertical wheel–rail contact force at the crossing against field measurements at three different train speeds. The model was later employed for the optimisation of crossing geometry [38] and elastic track properties [94].

In **Paper A** an alternative moving track model with two independent track masses (inner track mass and outer track mass) is proposed. The track masses in the model are decoupled in the vertical direction but rigidly coupled in the lateral direction, see Figure 7.5. The stiffness, damping and mass properties of the moving track model were determined by equating the static track stiffness, and the frequency and the magnitude of the damped fundamental resonance calculated with the FE model with the corresponding properties of the moving track model.

The moving track model has the advantage of simplicity and computational efficiency for simulating long-distance vehicle–track interaction. However, such models neglect the interaction between adjacent wheelsets that is transferred through the track structure [46]. Further, the physical properties of individual pad and fastening systems cannot be studied quantitatively and the influence of bending and torsion of the rails and sleepers is not accounted for. Typically, these models are only valid up to about 20 Hz, which is a severe restriction in the current application as the field measurements presented by Kassa & Nielsen [46] and Pålsson & Nielsen [47] have shown that the impact load at the crossing contains significant contributions at high frequencies ($\gg$ 20 Hz).
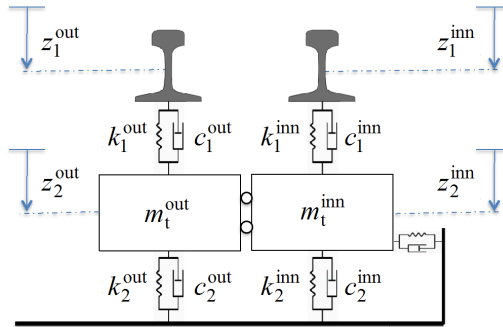

Figure 7.5: *Track model used in* **Paper A** *with vertically (in direction z) decoupled track masses (m_t) with separate stiffness and viscous damping for rail pad (k_1, c_1) and ballast (k_2, c_2). Superscripts indicate parameters of inner and outer rails*

7.4.2 Structural model with lumped parameters

For applications where the dynamic interaction is represented by higher frequencies than can be accounted for by a moving track model, continuous beam models of the track with lumped parameter supports are typically applied. Such models may account for the parametric excitation due to a vehicle moving on a discretely supported track as well as the periodic and discrete rail irregularities induced by rail joints [95, 96], unsupported sleepers [97] or S&C [98, 99].

For the rail model, Knothe & Grassie [75] concluded that the Euler-Bernoulli beam theory can be used for frequencies up to about 500 Hz. Kassa & Nielsen [46] suggested that this beam theory is sufficient for the simulation of vertical dynamic vehicle–crossing interaction. Thus Euler-Bernoulli beam theory has been used in **Paper A, Paper C** and **Paper D**. For higher frequencies, the Rayleigh-Timoshenko (R-T) beam theory is more accurate as it also accounts for the rotatory inertia of the beam cross-section and shear deformation, see e.g. Nielsen & Igeland [97]. The deformation of the rail cross-section is commonly assumed to be negligible but needs to be accounted for in calculations of rail noise, see [81, 90]. A computationally more efficient track model representing the rails by concentrated mass and stiffness matrices can be found in Bezin et al. [32].

The rail pad and track bed are commonly modelled by spring and viscous damper elements. The dynamic stiffness and damping parameters of the pad can be determined by tuning the calculated track receptance to the receptance measured in the field. The structural track model in the in-house software DIFF was developed by Nielsen & Igeland [97]. It has been extended for vehicle–turnout calculation by Kassa et al. [98], accounting for variation in rail cross-sections at the turnout, and considering frequencies up to 1500 Hz. Nielsen & Oscarsson [91] proposed a model accounting for the state-dependent characteristics of the elastic properties (such as the rail pad stiffness and the influence of unsupported sleepers). The method has been applied for the prediction of long-term degradation of railway track geometry due to accumulated differential settlement by Nielsen & Li [34].

The multilayered ballasted track model proposed by Zhai et al. [100] accounts for the interlocking and shear coupling effects among ballast particles by modelling the connection between ballast masses by shear springs and dampers. The model was extended to account for state-dependent properties by Sun et al. [101] to map a relationship between prescribed differential track settlement and rail/sleeper deflection. The study showed that sleepers are likely to become unsupported when the settlement amplitude is large or the settlement wavelength is short. The model was later modified by Guo & Zhai [102] to include an empirical ballast settlement model for predicting long-term track settlement and evolution of differential settlement. A recent review on train–track–bridge interaction, using structural models for the multilayered track substructure system, is given by Zhai et al. in [103].

In [99], Grossoni et al. described the track system as a three-layer discretely supported ballasted track, which includes the rail pad, the baseplate pad (installed between the rails and the sleeper) and the sleeper support resilient layers. An optimisation of track stiffness was performed for the crossing panel. The objective function used in the optimisation

was a weighted function based on predicted settlement, wear and rolling contact fatigue (RCF) of rail foot and rail head. The risk of settlement was evaluated based on calculated sleeper accelerations and sleeper–ballast contact pressure. The results showed that soft rail pads can reduce settlement, wear and RCF, but tend to increase stresses in the rail foot and rail head.

This type of structural track model has the advantage of accounting for spatially varying and state-dependent track properties. However, to account for the continuous variation in dynamic track properties in the switch and crossing panels, it requires the prescription of a large number of space-variant input data and a high number of DOFs, see for example [99, 104]. It may also be computationally expensive to incorporate a contact model such as Kalker's variational method to represent the non-linear wheel–rail contact mechanics in the S&C. In [105], Andersson & Dahlberg used an in-house software to simulate high-frequency vehicle–turnout interaction using a track model with parameters based on a FE model of the entire turnout. In [106], Alfi & Bruni proposed a model based on a three-dimensional FE representation of the track and a mixed rigid/flexible multi-body description of the wheelset. The equations of motion for these two subsystems were written separately, with wheel–rail contact forces acting as the coupling terms between the two sets of equations, and were integrated using a time-stepping algorithm. Another way to include the flexibility of the track is to translate the flexible components from a detailed FE model to a multi-body simuliation (MBS) software using a component mode synthesis method such as Craig-Bampton [107]. This method has been used in the EU-project *In2Rail* by Pålsson [108] to assess the sleeper–ballast contact pressure under the crossing with results similar to those observed in **Paper A** and **Paper D**.

7.4.3   Continuum models

Track modelled by continuum FE elements have been employed to account for the material behaviour of the track substructure (cf. [109–111] and **Paper B**) or rail and wheel (cf. [112]).

Lundqvist & Dahlberg [109] used the explicit FE method to simulate a rigid wheel moving along a 10-sleeper span track model including a simplified elasto-plastic material model of the ballast/subgrade. The influence of voided sleepers was assessed.

Wang & Markine [110] calculated track settlement in a transition zone by a two-step procedure. The vehicle–track interaction was simulated using a three-dimensional explicit finite element model with the rails modelled as beams supported by a layered continuum foundation. A simplified wheel–rail contact model was applied. A similar method was used by Varandas et al. [111] to analyse the principal stresses in the ballast during a train passage, where the track subtructure was modelled with continuum FE elements and moving wheel loads were applied on the rails modelled by beam elements.

The method used in **Paper B** takes a similar approach, where the calculated wheel–rail contact force calculated in **Paper A** is mapped to the track structure and a continuum 3D FE model of the track substructure is employed to evaluate the stress-strain condition in the track substructure including the ballast, sub-ballast and subgrade, see

Fig. 7.6.

In [112], Pletz et al. presented a dynamic FE model to study RCF on the crossing nose, with both the wheel and the crossing rail modelled by solid elements. The approach can be used to investigate non-linear material behaviour of the wheel and the rail, but due to high computational cost a limited simulation distance needs to be considered. Coupling procedures, where the prestress and deformation due to wheel load were solved using an implicit FE code before the dynamic simulation was continued with an explicit FE code were employed by Cai et al [113] for analysing stresses in rails at rail joints and by Xin & Markine for predicting RCF in a railway crossing [114].

The FE models using continuum elements and explicit time integration scheme have several advantages. The continuum element formulation for the track superstructure and substructure allows for a direct incorporation of non-linear and more advanced material models. If the response of the track substructure is of main interest, the models often constitute a simplified representation of the vehicle–track interaction. For vehicle–turnout interaction, where the dynamic impact load at the crossing transition is of interest, a detailed modelling of the wheel and crossing geometry is important. Due to the required extensive computational effort, a limited length of the track needs to be considered.
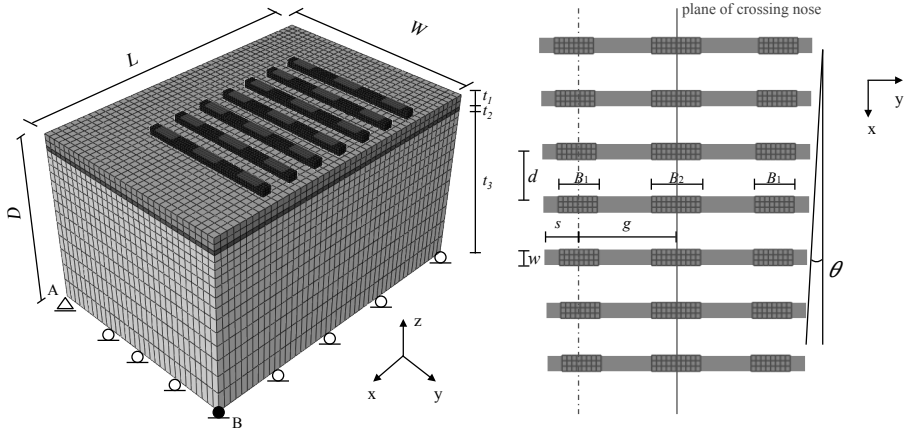
Figure 7.6: *Illustration of FE model used in* **Paper B**. *Finite element discretisation, boundary conditions and component dimensions are shown. Ballast thickness t_1, sub-ballast thickness t_2 and subgrade thickness t_3. Track substructure dimensions W, L, D. Top view $(x-y$ plane) of the track structure; sleeper width w, sleeper spacing d, baseplate width at the outer rails B_1, baseplate width at crossing nose B_2, and crossing angle θ*

7.5 Wheelset models

Depending on the frequency of interest, different levels of detail of the vehicle model should be included in the simulation of vehicle–track interaction. Knothe & Grassie [75] concluded that the vehicle dynamics is dominated by frequencies below 20 Hz. At higher frequencies, a rigid wheelset model can satisfactorily represent the vertical excitation of the track. This is due to the fact that the primary and secondary suspensions of the vehicle isolate the bogie and car body from the wheelset. The unsprung mass, which comprises the wheelset, bearings, brake discs, axle-hung traction motor and gear box is the main contribution to the vertical dynamic excitation between wheelset and the track at frequencies above 20 Hz. For lateral vehicle dynamics, and for models to predict rail corrugation or noise, a model that includes the resonant behaviour and lateral flexibility of the wheelset may be required [75]. The modelling of a flexible and rotating wheelset was addressed by Torstensson [90].

In the mid- and high-frequency range (above 50 Hz), Popp et al. [115] suggested that simple rigid multi-body models are sufficient for the modelling of the car body and bogie as the dynamic behaviour of the car body and bogie is decoupled by the soft secondary suspensions. The elasticity of the wheelset should be taken into account for solving acoustic problems. In many multibody dynamics software, such as GENSYS [92], the rigid-body representations (mass, moment of inertia, position of centre of gravity) of the car body and bogie are commonly adopted, where spring and viscous damper elements are used to interconnect the bodies. Large rigid-body translations and rotations of the bodies can be treated. In **Paper A** and **Paper B**, the turnout is subjected to freight traffic represented by a model of one car body and two bogies. Each bogie has non-linear primary and secondary suspensions and two wheelsets.

In **Paper C**, a single rigid wheel model with a linear primary suspension (spring and viscous damper) is applied. In **Paper D**, a flexible wheelset model is included, see Figure 7.7(a). The calculated point receptances for the rigid wheelset model and the flexible wheelset model are compared in Figure 7.7(d). It is observed that the rigid model is a satisfactory approximation of the flexible wheelset model up to about 150 Hz. The point and cross receptances of the flexible wheelset model for excitation at the nominal wheel–rail contact point of one wheel have also been studied, see Figure 7.7(e). The fundamental resonance at 19 Hz, where the wheelset is vibrating on the primary suspension stiffness, is the same for the rigid and flexible wheelset models. The lowest symmetric bending mode of the wheelset is at 95 Hz, while the lowest anti-symmetric bending mode is at 184 Hz, see Figures 7.7(b) and (c). It is observed in **Paper D** that the influence of the wheelset flexibility on the calculated sleeper–ballast contact pressure is moderate.

(a)   (b)   (c)

(d)   (e)
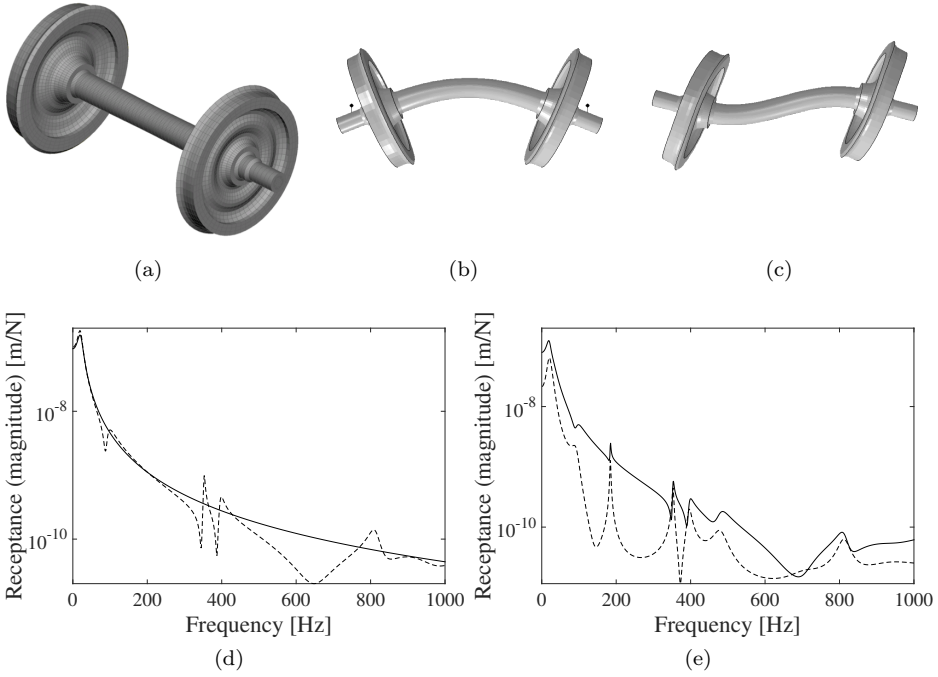
Figure 7.7: *(a) Flexible wheelset model of continuum hexahedral elements presented in **Paper D** (b) lowest symmetric mode of the wheelset at 95 Hz, (c) lowest anti-symmetric bending mode at 184 Hz, Examples of (d) point receptance of the rigid wheelset model (——) and flexible wheelset model (- - -) and (e) point (——) and cross (- - -) receptances of the flexible wheelset model, for excitation at the nominal wheel–rail contact point*

7.6 Wheel–rail contact models

The wheel–rail contact constitutes the coupling between the vehicle and track subsystems in the simulation of dynamic vehicle–track interaction. To accurately account for the non-linear characteristics of the contact and the high contact stiffness, very small time steps are required, which is a main reason for the high computational cost [90]. A thorough discussion on the topic of efficient modelling of wheel–rail contact in vehicle dynamics simulations can be found in Sichani [116].

According to Sichani [116], the general wheel–rail contact problem constitutes two parts: (1) detecting the number of contact points and determining the size and shape of the contact area (geometric part), (2) calculating the contact stress and material deformation (constitutive part). The contact geometry is determined by the wheel and rail profiles and the local deformation in the wheel-rail contact. The number and locations of contact points and the corresponding contact angles on the wheel and rail define the positions and orientations of the contact forces [6]. The constitutive part solves the distributions of the contact pressure (normal compressive stress) and the tangential (shear) stress over the contact patch [116]. The wheel–rail contact geometry problem can either be solved in each time step during the time integration (online), or determined in advance using a pre-processor (reading of a look-up table) [6].

7.6.1 Look-up table

When using a look-up table, the contact problem is solved in advance in a preprocessing step and the results are tabulated [117]. The contact geometry problem is treated as a two-dimensional problem. By assuming zero wheelset yaw angle, linear elasticity and a smooth contact surface, the contact problem is solved for different relative lateral wheelset displacements. The precalculated contact geometry functions are saved as look-up tables. During subsequent time integration, a linear interpolation of contact geometry for the current wheel position is made for each time step [6]. This enables the wheel–rail contact problem to be solved more efficiently.

This method is adopted for example in the commercial software GENSYS [92] in its pre-processor KPF (abbreviation for "contact point functions"). In KPF, an equivalent Hertzian contact model (see Section 7.6.2) is fitted to the contact conditions determined by the relative lateral displacement between wheel and rail and for each combination of wheel/rail profiles at sampled locations [4]. The tangential contact problem is solved using the FASTSIM algorithm (simplified theory according to Kalker [118]). The contact model accounts for two-point contact situations. The method has been described and used for the simulaton of dynamic vehicle–turnout interaction in works by Kassa [6] and Pålsson [4] and also in **Paper A** and **Paper B**. To account for the variation in contact geometry along the turnout, the cross-section of each rail is sampled at several positions along the turnout. The sampling distance is determined by the rate of variation of rail profile. In the crossing panel in **Paper A**, the sampling distance between two cross-sections is 50 mm.

However, the magnitude of the wheel–rail impact load at the crossing transition is

very sensitive to the wheel transition point, at which the wheel moves between wing rail and crossing rail [4]. The multiple point contact condition shown in Figure 7.2 (here a two-point contact) is an indication of when the wheel transition occurs. The linear interpolation of contact geometry between two consecutive profiles can lead to errors in predicting the exact transition point. To this end, an online solver is considered to present a more accurate prediction of the magnitude and position of the time-variant contact force during the transition of the wheel in the crossing panel.

7.6.2 Hertzian contact

For normal wheel–rail contact problems, Hertzian contact theory [119, 120] is commonly used. It formulates the contact stiffness based on the material properties and the radii of curvature in the contact point. Some of the assumptions in Hertzian theory are: (1) The materials in contact are isotropic, linear elastic and quasi-identical. (2) The bodies in contact can be approximated as elastic half-spaces, meaning that the contact area is small compared to the contacting bodies. (3) The radii of curvature of wheel and rail profiles within the contact patch are considered to be constant and the resulting contact area is elliptical. Only non-conformal contact is considered. When the vertical wheel–rail contact force resulting from normal contact along a straight track (standard rails) is of interest, Hertzian theory can be used to provide fast solutions. Hertzian theory has been applied in **Paper C** and **Paper D** for wheel–rail contact along the outer rail of the through route in a turnout.

For wheel–rail contact on the crossing rail in a vehicle–turnout simulation, some of the assumptions listed above are violated: (1) The linear elastic material assumption is violated as severe plastic deformation has been observed in the crossing nose due to severe impact loads caused by non-optimal wheel–rail contact geometry in the transition zone, see Skrypnyk et al. [121]. (2) The half-space assumption is not valid. For contact on the crossing rail, the smallest radius of rail curvature is similar to the largest semi-axis of the contact area. However, Yan & Fischer [122] and Wiest et al. [123] found that the half-space assumption can be used for crossing rail contact as long as no plastic deformation of the material occurs. (3) The assumption of constant radii is violated when the wheel flange is in contact with the rail gauge corner causing conformal contact and a non-elliptic contact area.

As stated above, the crossing transition may result in multiple contact positions. In this case, a model that accounts for the case of multiple-point and non-Hertzian contact is required.

7.6.3 Kalker's variational method

Various categories of approximate solutions for solving multiple-point contact problems exist [116, 118, 120, 124–127]. In [124], Pascal and Sauvage proposed a set of Hertzian ellipses and then further approximated the contact by a single equivalent ellipse to replace the multiple and non-Hertzian contact patches. This method has been shown to be adequate for static stress analysis but less suitable for dynamic simulations [126]. Another

type of method presented by Piotrowski & Kik [126] and by Ayasse & Chollet [125] estimates the contact area from the interpenetration area that is obtained by virtually penetrating the two undeformed surfaces. In **Paper C** and **Paper D** of this thesis, Kalker's variational method [127] has been applied. For a discussion and description of the other non-Hertzian methods, see Sichani [116].

Kalker's variational method, also called Kalkers complete theory, is the preferred alternative for the calculation of non-Hertzian and multiple-point wheel–crossing contact. It deals with the normal and tangential rolling contact problem for arbitrary geometries as long as the half-space and linear material assumptions are valid, and it provides both the steady-state and transient solutions.

The method is based on the discretisation of the Boussinesq-Cerruti integral equations using a set of rectangular elements, in which the surface traction in each element is taken as constant [127]. It formulates the contact problem as a minimisation of an energy potential over a potential wheel–rail contact area moving at vehicle speed in the longitudinal direction [81]. The potential contact area, which is larger than the actual contact area, is meshed by rectangular elements (boundary element method) and divided into two sets: the in-contact set, where the elements are in contact, and the active set, where the elements are not in contact. An initial assumption is made about which elements belong to the active set. The wheel–rail contact area and the contact pressure distribution are solved by an iterative procedure. In each iteration, elements with a negative pressure value are removed from the in-contact set to the active set, until all the remaining elements in the in-contact set have positive pressure values, see Pieringer [81]. The tangential stresses in each element is calculated after obtaining the contact patch and pressure distribution from the normal contact solution. Kalker implemented this theory in his computational code CONTACT, which has been further developed by Vollebregt [128–131].

Pieringer [81] developed a time-domain model of dynamic wheel–rail interaction based on the Green's function approach for the vehicle and track subsystems in combination with an online implementation of Kalker's variational method to solve the non-Hertzian, and potentially multiple, wheel–rail contact. This method has been applied for the vehicle–crossing contact model in **Paper C** and **Paper D**, in which only the normal contact has been considered. The contact geometry and contact pressure for a hollow worn wheel running on the crossing rail in the facing move of the through route (no lateral wheel displacement) is demonstrated in Figure 7.8.

7.6.4 Finite element models

A more general solution to the rolling contact problem is based on the finite element method. In FE-based approaches, the contact bodies are discretized by continuum elements. The contact constraints are imposed and three systems of equations are solved in order to determine the nodal contact forces: the equations of motion, the compatibility equations (which relate the strains to the displacements) and constitutive equations (which relate the stresses to the strains). The Lagrangian formulation is a common way to describe structural deformation in solid mechanics. The reference coordinate system
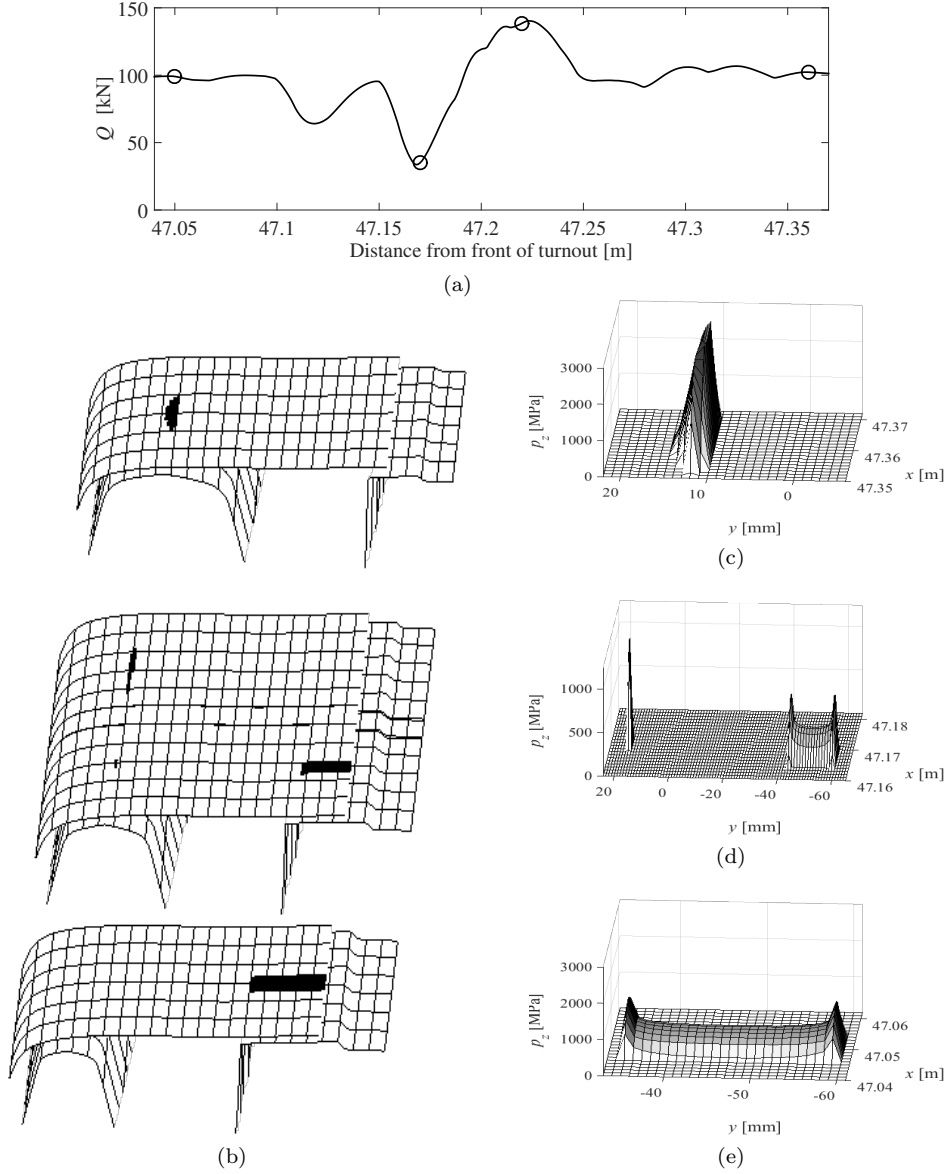
Figure 7.8: *Illustration of contact geometry and contact pressure between wheel and rail during wheel transition from wing rail to crossing. Simulation performed for traffic (S1002 wheel profiles) in facing move of through route of a 60E1–760–1:15 turnout. (a) Vertical wheel–rail contact force (circles mark selected points in the time history). Contact geometries shown in (b) for contact at $x = 47.05$ m, $x = 47.17$ m, $x = 47.22$ m and $x = 47.36$ m from front of turnout. Vertical wheel–rail contact pressure shown for contacts at (c) $x = 47.22$ m, (d) $x = 47.17$ m and (e) $x = 47.05$ m. From **Paper C***

36

in a Lagrangian formulation is the material coordinate system, meaning that the mesh nodes are connected to the particles of the material. To obtain accurate stresses in the wheel–rail contact area, a high resolution of the mesh is required in this area. It is mainly used for static problems or simulation of dynamic vehicle–track interaction along a short distance, see e.g. Pletz et al. [112]. Alternatively, a so-called Arbitrary Lagrangian-Eulerian description that allows for localised mesh refinement can be employed to reduce the computational cost in a transient rolling contact simulation. A thorough description of this subject was addressed by Draganis [132].

8 Modelling of track settlement

As described in Section 4, the granular layers (ballast and sub-ballast) accumulate permanent deformation (settlement) due to gradation change, particle breakdown, volumetric compaction and abrasive wear. The subgrade settles due to plastic volume change and progressive shear failure.

The track substructure undergoes consolidation and increases in stiffness. Li & Selig [133] categorised empirical models of elastic moduli for fine-grain soils. A review on the material modelling of elastic modulus of unbounded aggregates of granular material is given by Lekapr et al. [134].

According to Dahlberg [15], in terms of permanent deformation of granular materials, no generally accepted damage or settlement model has been established. In order to predict settlement and schedule maintenance actions, various methods for the modelling of track settlement have been investigated. In this section, a review on track settlement modelling will be presented with a focus on settlement in the ballast layer. First a review will be given on some of the empirical settlement models. Then, modelling of ballast particle behaviour using a microscopic approach will be surveyed. In the third section, literature on constitutive models developed for long-term behaviour of granular material will be reviewed and the model used in this thesis will be described. In the fourth section, integrated procedures that combine an empirical model with a discrete element model or a constitutive model for the simulation of accumulated permanent deformation for a large number of load cycles are discussed. At last, to predict the long-term settlement and its effect on train–track interaction, an iterative calculation scheme is needed. Some examples of such a scheme, including the one used in this thesis, will be illustrated.

8.1 Empirical settlement models

In railway applications, the early work of track settlement modelling has been mainly empirical. The empirical models consider the track substructure as a whole without separating the track bed layers. Most empirical models formulate settlement as a function of the number of load cycles to capture the two phases of settlement (the short- and long-term settlement).

The most widely used empirical models have different types of formulation with respect to the number of load cycles: the logarithmic models and the power models. The threshold models, on the other hand, have been formulated with respect to load magnitude for a given number of load cycles.

8.1.1 Logarithmic model

The track settlement models proposed by Alva-Hurtado & Selig [7, 17], Shenton (1978) [135], Hettler [136] and Indraratna [137] feature a logarithmic growth of the long-term settlement, see for example Equation 8.1 copied from Shenton (1978) [135].

$$\varepsilon_N = \varepsilon_1(1 + C\log N) \tag{8.1}$$

where ε_1 is the predicted permanent strain after the first load cycle, C is a dimensionless parameter controlling the rate of settlement growth, N is the number of load cycles, and ε_N is the accumulated permanent strain after N cycles. The permanent deformation (settlement) of the ballast is then calculated based on the product of accumulated permanent strain and ballast thickness.

One of the earliest settlement models was established by the Office for Research and Experiments of the International Union of Railways (ORE) [138]. The method evaluates the settlement as a function of tonnage. Properties of individual track components are not considered. The model was later improved by Shenton (1978) [135] to take into account the effect of sleeper spacing. The initial permanent strain was determined by the porosity and principal stresses of the ballast measured in a triaxial test.

The model by Alva-Hurtado & Selig [17] assumes that the ballast deformation starts from an uncompressed state. It accounts for axle loads of various magnitudes by converting the higher load magnitudes into lower load magnitudes with a modified number of equivalent load cycles. The variation of load magnitude is incorporated by varying the permanent strain after the first cycle.

The model by Hettler [136] calculates the initial settlement based on an equivalent load amplitude that is equal to the mean load of N load cycles. The data in the Hettler model [136] were based on measurements on a scaled sleeper track model.

8.1.2 Power model

The power model typically takes the form

$$\varepsilon_N = AN^b \tag{8.2}$$

where A, b are dimensionless coefficients and N is the number of load cycles, ε_N is the accumulated permanent strain. Shenton (1985) [18] derived the power model based on a triaxial test with a large number of load cycles (up to 10^6).

$$\varepsilon_N = AN^{0.2} + BN \tag{8.3}$$

The coefficients A, B are related to the average axle loads, tamping lift force, sleeper size/type/spacing and ballast/sub-ballast/subgrade conditions. For high load amplitudes, Shenton found the settlement to be proportional to the fifth power of the number of load cycles, while for moderate load amplitudes, the settlement is a linear function of the number of load cycles. Based on triaxial tests, Shenton concluded that the magnitude of the load dominates the level of track settlement, implying that for many railway lines, it is the higher loads that causes the track settlement [15]. An empirical equation to calculate an equivalent load to represent the case of varying axle loads was also suggested. Similar power models for fine-grain soil were derived by Li & Selig [12], with the coefficient A expressed as the ratio of dynamic deviatoric stress σ_d and static soil strength σ_s:

$A = a(\sigma_d/\sigma_s)^m$, where a and m are material parameters. The empirical models used in some Japanese settlement studies are also included in this category [139]. In 1995, one of the most famous empirical models was proposed by Sato [16]. It reads

$$z = \gamma(1 - e^{-\alpha N}) + \beta N \qquad (8.4)$$

where z is the track settlement, N represents the number of load cycles or the tonnage. The first part of Equation 8.4 represents the initial short-term settlement, while the second part represents the long-term settlement. The parameter γ and α control the short-term deformation. The parameter β, which controls the long-term deformation, is considered to be influenced by stone integrity, sleeper–ballast contact pressure, ballast vertical acceleration and contamination and drainage conditions. The value for β is higher for new gravels than for crushed stones and higher for clean and/or dry ballast than for contaminated and/or wet ballast. This implicates that a newly constructed ballasted track degrades faster than a track that has had a long service life. The value for β is also proportional to the energy that is transfered into the track substructure. Mathematically, it is proportional to the square of the sleeper velocity, and proportional to the product of sleeper–ballast contact pressure and ballast vertical acceleration. This indicates that track subjected to high dynamic wheel–rail contact forces are prone to severe track settlement.

The linear long-term settlement growth in Equation 8.4 has the same linear growth with number of load cycles as the second part of the Shenton (1985) model in Equation 8.3. The model has been validated by a sliding-stone laboratory test and a field test carried out in Japan. The short-term settlement is observed to be small in magnitude compared with the long-term one. Similar exponential models have been proposed by Sun & Indraratna [63] and Guérin [140].

Dahlberg [15] commented that as the long-term growth is modelled differently in the power model and the logarithmic model, the discrepancy between the two models might be large, especially if the parameters in the equations are determined based on a small number of load cycles but used to determine the settlement for a large number of load cycles. Recently, Abadi et al.[141] re-assessed exisiting empirical models in a large-scale laboratory test. The settlement for two different types of ballast material after one million load cycles was evaluated. The differences between the model prediction and the measurement were related to the variation in load amplitude and ballast material quality from which the empirical models were derived. Grossoni et al. [142] also summarised the main empirical models and their test methods. In their study, the empirical models by Sato (1995) [16] (Equation 8.4) and Guérin [140], for the cases of three levels of track support stiffness and three traffic types, were compared using an iterative simulation procedure. It was found in [142] that the model by Sato is more sensitive to train speed than the Guérin model. The difference was explained by the different test methods (field measurements by Sato versus triaxial test by Guérin) and the different traffic conditions considered (heavy freight traffic by Sato versus high-speed lines by Guérin) on which the two models were based.

8.1.3 Threshold function

In the literature, it is generally agreed that permanent deformation (settlement) does not occur when the load magnitude is below a certain threshold value. This threshold value can be considered as a yield limit of the ballast.

In 1997, Sato [143] proposed an alternative empirical model to explicitly account for the magnitude of the traffic load:

$$z = a\langle p - b\rangle^n \qquad (8.5)$$

where p is the sleeper–ballast contact pressure and the Macaulay brackets are defined as $\langle\bullet\rangle = 1/2(\bullet + |\bullet|)$. The parameter $b\,[\mathrm{N/m^2}]$ is the threshold sleeper–ballast contact pressure below which track settlement does not occur. The influence of load magnitude on settlement is determined by the power n. The settlement data was based on field measurement after 10 000 load cycles at constant load levels. Based on *in-situ* measured data from Sato (1997) [143], the formulation was extended and recalibrated by Dahlberg [15]. The revised model reads:

$$z = 0.02\langle P - 95\rangle + 3.0 \times 10^{-10}\langle P - 95\rangle^n \qquad (8.6)$$

where P is the measured sleeper–ballast contact force. Here $P = pA_{\text{sleeper}}$ and A_{sleeper} is the sleeper base area. For moderate values of sleeper–ballast force P, the settlement grows almost linearly with increased loading. For higher values of the contact force, there is a non-linear region where the settlement depends strongly on the force magnitude (proportional to the fifth power of the sleeper–ballast contact force). In [15], it is suggested that the nonlinear region indicates that there might be different degradation or failure mechanisms involved in different load ranges. For example, there might be abrasion and compaction of the ballast particles in the lower load range and fracture of ballast particles in the higher range. In **Paper A**, using the model in Equation 8.6, settlement after 10 000 axle passages of the same vehicle type is extrapolated based on the simulation of one vehicle passage. Note that the threshold contact force F_t (here 95 kN) is generally dependent on the number of load cycles due to material densification. Implementation of this model implies that the two-phase settlement mechanism is not considered.

8.2 Discrete element models

The discrete element method (DEM) has been used to investigate the inhomogeneous effects of ballast at particle level. The discrete element method considers the granular layers (ballast, sub-ballast and subgrade) as an assembly of a finite number of particles. In each time step, the system equilibrium is determined by accounting for the normal and tangential contacts between the particles. This type of method is able to capture local deformations and heterogeneous grain movements, but it requires a large number of elements in a representative volume and considerable computation time [67]. Results from the DEM are sensitive to the initial stochastic arrangement of the particles, and thus

the simulation needs to be repeated with different initial conditions to achieve reliable mean values [144].

The DEM has been used to determine the elastic moduli of granular media [145, 146], to investigate inter-particle forces during construction and tamping [147], particle interlocking, breakage, wear and degradation [148–151], and to generate constitutive material models for settlement [152–154].

8.3 Constitutive models

The use of a continuum model approach can be an attractive alternative for the modelling of long-term accumulated track settlement. To simulate the response of a material subjected to cyclic loading, there are both conventional models that account for the hysteresis of the loading and unloading, and cycle-domain models that rely on the load amplitude and material status after loading. A review on material modelling and plastic deformation of unbounded aggregates of granular material was given by Lekarp [155]. In this section, conventional constitutive models for granular material will be briefly disussed followed by a short review of cycle-domain shakedown models. The Cycle Densification Model (CDM) developed by Suiker & de Borst [156], which is applied in **Paper B**, will be described in some more detail.

8.3.1 Conventional models

Reviewed by Jacobsson & Runesson [157], the response of a granular material is traditionally described by a constitutive model with pseudo-elastic or hypo-elastic material properties that account for the gradual change of the elastic moduli [24, 133] and the non-tension effect [158]. The non-tension effect refers to the stress-free situation when the granular material is subjected to a tensile force. The plastic deformation under monotonic compressive loading has been modelled mainly by elasto-plastic [159–164] or hypoplastic models [165–167]. Many of these models were initially developed for fine-grained soils, such as clay or sand. The confining pressure and shear behaviour of ballast particles were studied in [55, 168]. Constitutive models have been derived for ballast settlement incorporating particle breakage by Indraratna [169, 170].

8.3.2 Cycle-domain shakedown models

A conventional constitutive model formulated in terms of the rates of stress and strain requires many numerical increments for each load cycle simulation. When simulating many load cycles, the numerical error may become excessive and the calculation effort substantial [171]. The material parameters of such models need to be calibrated against cyclic experimental data with complete loading and unloading history. Laboratory data for calibration is easier to obtain for smaller granular materials, such as sand, but is more difficult for large granular particles, such as railway ballast.

An alternative approach for efficient settlement modelling is to use a constitutive model that evaluates the progressive accumulation of plastic strains under repeated load-

ing in the cycle domain. For each load cycle, the shakedown concept is applied to obtain the material response with respect to the load level. If the magnitude of the applied loads exceeds a limit value (shakedown limit), plastic strains are accumulated progressively under repeated loading. On the other hand, if the applied loads are lower than this shakedown limit, the growth of plastic strains will eventually level off and the material attains a state of shakedown by means of adaptation to the applied loads [60].

This concept was introduced by Sharp [172] for the modelling of a fine-grain unbounded granular material (sand or clay), and applied experimentally and numerically for pavement material, see Lekarp & Dawson [60], Werkmeister et al. [61], Garcia-Rojo & Herrmann [62], Collins & Boulbibane [173] and Chazallon et al. [174]. The method has been extended to the application of ballast by Suiker & de Borst [156] and by Jacobsson [157]. Here the method developed by Suiker & de Borst will be illustrated.

Cycle Densification Model

The Cycle Densification Model (CDM) developed by Suiker & de Borst [156] was motivated by experimental findings of railway ballast degradation. The resulting CDM is formulated as a viscoplastic model where the rates of the variables are described as their change per unit cycle N. In the CDM, permanent strain will only develop if the stress amplitude in a given load cycle exceeds a certain threshold value, see Figure 8.1. The stress and/or strain amplitudes are the input variables, which result in a possible evolution of plastic strain per cycle. The CDM captures only the maximum plastic deformation generated by the magnitude of the train loading during each load cycle.

The driving mechanism is decomposed into volumetric compaction and frictional sliding. The pressure-dependent elastic modulus is also accounted for. The threshold value is defined by a Drucker-Prager frictional shakedown criterion and a shakedown criterion in compression. Both shakedown functions are allowed to harden in a similar way as ordinary yield surfaces. The deformations are distinguished by four response regimes,
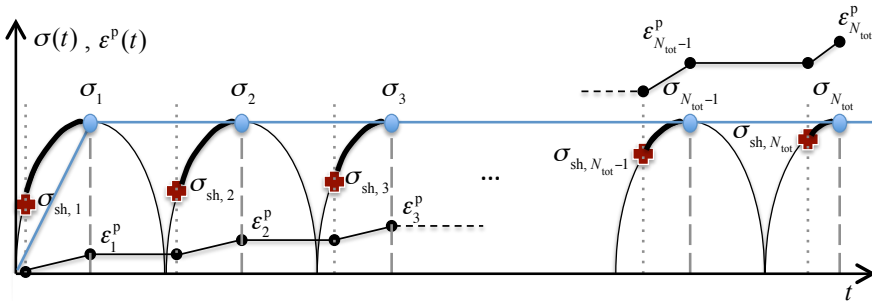
Figure 8.1: *Schematic illustration of how plastic strain $\epsilon^{\mathrm{p}}(t)$ can accumulate during cyclic stress-controlled (with constant amplitude) loading $\sigma(t)$. In the illustration, effective amplitude stresses σ_N, shakedown threshold stresses $\sigma_{\mathrm{sh},N}$ and the corresponding accumulated plastic strain ϵ^{p}_N ($N = 1, 2, \cdots N_{\mathrm{tot}}$) are shown. From **Paper B***

which are: (1) shakedown, (2) cyclic densification, (3) frictional failure and (4) tensile failure, see Figure 8.2

In **Paper B**, the CDM is used and explored for three-dimensional modelling of ballast settlement with the objective to account for longitudinal variations in load, structure and material properties. In this paper, settlement is first predicted for a laboratory test case where measured data for a straight track subjected to quasi-static cyclic loading is available. Then, an analysis of settlement in a crossing panel is performed and the spatially varying (differential) settlement due to dynamic impact at the crossing nose is studied.

The advantage of using a cycle domain constitutive model for simulating settlement is that the material parameters can be calibrated based on the material status after each load cycle, and that the experimental data for the full time history of loading and unloading is not required. A challenge of using such a model in railway applications lies in the representation of the structural loading. The feature where, as in the time domain, the maximum loads amplitudes on adjacent sleepers are not reached at the same time is not accounted for in the CDM. This means that the amplitudes of the loads on the sleepers must be modified before adopting the CDM to compensate for this fact. In **Paper B**, each sleeper load is multiplied by a scale factor. Here this scale factor was determined by comparing calculated track settlement with the corresponding settlement measured in the CEDEX full-scale test rig [66].
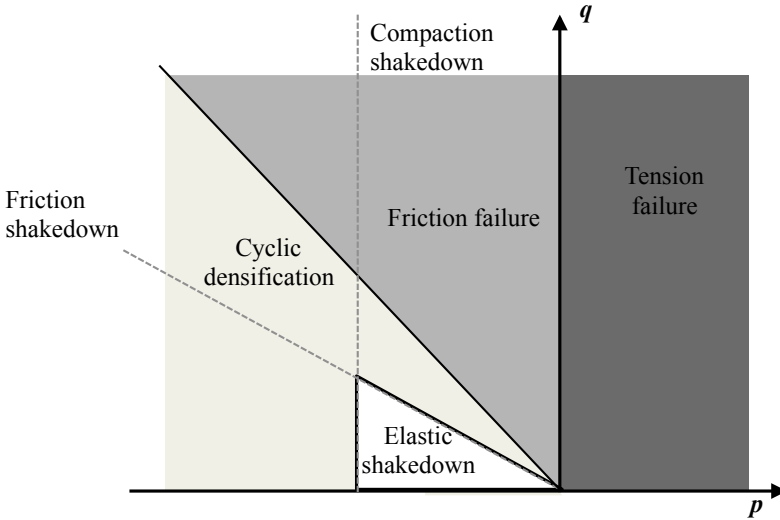

Figure 8.2: *Various response regimes in the $p - q$ plane due to cyclic loading, where p is the hydrostatic stress invariant and q is the deviatoric stress invariant (von Mises stress). The stress ratio $-q/p$ is a measurement of isotropic frictional failure under three-dimensional stress conditions. From [67]*

8.4 Integrated procedures

To improve computational accuracy and efficiency, and to combine the strengths of various approaches, integrated computational procedures to predict the plastic deformation for the first cycle(s) and extrapolate the trend to the subsequent cycles have been proposed in various studies [152, 154, 175, 176].

In the work of Karrech et al. [152], a combination of DEM and empirical model was used to predict long-term settlement. The DEM was applied to establish a trend function in terms of settlement for the first k cycles. The empirical model by Shenton (1985) [18] was then used for the extrapolation. Based on the updated empirical model, new particle positions were extrapolated and used in the new loop of the DEM calculation.

The Disturbed State Concept (DSC) was proposed by Desai et al. [175] and applied to simulate ballast settlement under cyclic loading for the first 10–20 cycles. The total accumulated plastic strain was extrapolated from the simulated plastic strains via an empirical model. A similar approach was taken by Pasten et al. [177].

In the work by Niemunis & Wichtman [176, 178], the given traffic load history was decomposed into load collectives of different amplitudes. A hypoplastic model was then used to calculate the plastic strain for a controlled load cycle. The plastic strain was assumed to be the same for all loads in the same load collective. The settlement was calculated as the accumulated plastic strain after applying all the load collectives. The order of applying the different load collectives was shown to have a little effect on the accumulated plastic strain.

8.5 Iterative scheme

The cycle-domain constitutive models and integrated procedures can be used to simulate material plastic deformation for a large number of load cycles with a relatively good accuracy and efficiency. However, the plastic deformation is calculated for a prescribed load collective. To account for that the magnitudes of the loading may be influenced by the accumulated deformation, an integrated approach is required involving also repeated simulations of the dynamic vehicle–track interaction. Some examples of this approach are reviewed below.

Varandas et al. [179] proposed an iterative methodology to determine track settlement in a transition zone. In the first step, the sleeper–ballast contact forces were calculated for various types of vehicles at different vehicle speeds using a structural track model. Based on the forces transmitted to the ballast, the settlement generated under each sleeper of the track by each vehicle axle was determined using an empirical model. The traffic loading was assumed to be constant in the short-term until accumulated settlement at any given sleeper reached a limit value. A new dynamic simulation was then performed with the updated longitudinal level and track configuration. It was found that the loading sequence did not influence the accumulated settlement. In the work of Wang & Markine [30], a 3D FE model was employed to compute the dynamic vehicle–track interaction in a transition zone. The ballast stress obtained from the FE model was used as input to an

empirical model (Sato model from 1997 [143]) for the calculation of track settlement. The track geometry was updated after every N cycles. In the work by Grossoni et al. [142], an iterative process connecting vehicle–track interaction and empirical models has been used to assess the influence of spatial variability of track stiffness on the evolution of differential track settlement. The influence of parameters including unsprung mass, vehicle speed, support stiffness characteristics and standard deviation of rail irregularities have been assessed. It was found that the most influential parameters on ballast deterioration rate are the spatially varying track stiffness and the unsprung mass.

In **Paper A**, the iterative methodology for the prediction of track settlement in railway turnouts includes simulation of dynamic vehicle–track interaction using a multibody dynamics software, calculation of sleeper–ballast contact pressure using a finite element model and prediction of track settlement using an empirical model. The accumulated track settlement at each sleeper and the resulting vertical track irregularity along the turnout is used as input in the next step of the iteration, see Figure 8.3. The methodology was improved and implemented by Nielsen & Li [34] to calculate the long-term degradation of longitudinal level at a rail joint.
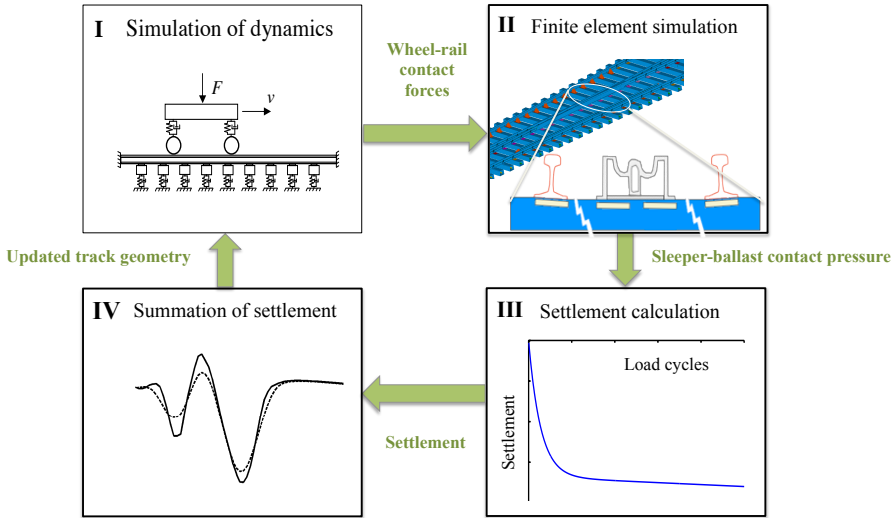

Figure 8.3: *Illustration of iterative scheme in* **Paper A** *for prediction track settlement*

9 Maintenance methods and mitigation measures

In this chapter, maintenance methods and mitigation measures to reduce track settlement will be described.

9.1 Track substructure maintenance

The two most common maintenance methods to reduce vertical track irregularities due to accumulated settlement are tamping and stoneblowing [67, 180].

In the case of tamping, each individual sleeper is lifted to a prescribed level. The steel spikes of the tamping unit are used to squeeze the ballast particles below and around the sleeper and to stablise them through vibration. At the end of the tamping procedure, the ballast is supposed to be at a height that can support the desired track geometry and the sleeper is repositioned to the adjusted ballast layer [67], see Figure 9.1. Tamping is effective to correct ballast geometry and track level. However, this correction is accompanied by undesirable disturbances of the ballast structure, breaking of ballast particles and intermixing of ballast and sub-ballast [67], leading to fouling and poor drainage [180]. Sometimes, the tamping action also loosens the ballast below the sleeper as well as at the shoulder, creating partially supported (voided) sleepers directly after tamping [181]. Preventive measures, such as lifting the ballast higher than its original level and recompacting the ballast directly after tamping have been suggested to enhance the durability of tamped ballast track [180].

An alternative to tamping is stoneblowing where small stones (14–22 mm) are blown into the void below the lifted sleeper to support the sleeper at its original position, see Figure 9.2. The advantage of stoneblowing is that the original ballast layer is minimally disturbed, without squeezing or crushing the ballast stones [67]. It can also be performed at frequent intervals to prevent ballast settlement [180]. The study by Sol-Sanchez et al. [182] shows that the stone-blowing process is more effective than tamping in maintaining the track geometry and reducing the frequency of required maintenance actions. It also leads to a more stable short- and long-term mechanical performance of the section, as well as resulting in lower degradation of ballast and substructure, see Figure 9.3.

9.2 Mitigation measures

Design and maintenance measures to slow down the deterioration of ballasted railway track are reviewed by Sol-Sanchez and D'Angelo [180]. Elastomeric products, such as rail pads, USP, under-ballast mats (UBM), sub-ballast mats (SBM), and geogrid (or geotextile) reinforcement can be used to design a transition zone with a desired (smoother) variation in track stiffness. Lazorenko et al [13] reviewed mitigation measures for the stability of soil foundation in heavy-haul railway tracks.

Rail pads are elastic elements installed between rails and sleepers to filter the high-frequency contributions of the dynamic forces from the wheel–rail interface, and thus

reduce pressure at the sleeper–ballast interface. Rail pad stiffness in the range 80–125 kN/mm are commonly used in modern railway tracks [180]. The effect of low-stiffness rail pads in attenuating impact loads on the crossing has been reported in [47, 99, 183, 184]. The effect of rail pad stiffness has been further studied in **Paper D**. It is found that if the rail pad is already sufficiently soft, further reducing its stiffness has a limited effect on reducing the sleeper–ballast contact pressure.

Under sleeper pads (USP) have been introduced at the sleeper/ballast interface to
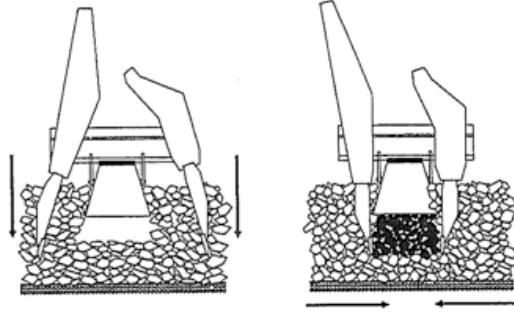

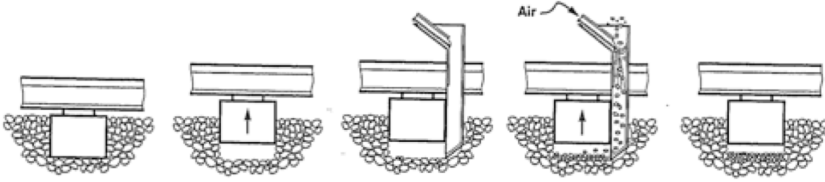Figure 9.1: *Tamping procedure. From [7]*
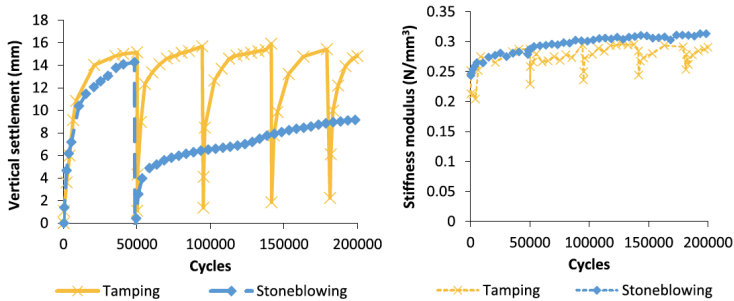

Figure 9.2: *Stoneblowing procedure. From [7]*

Figure 9.3: *Comparison between effects of tamping and stoneblowing on ballast performance. (left) Ballast settlement rate is lower after stoneblowing than after tamping, and (right) vertical track stiffness is more homogeneous after stoneblowing than after tamping. From [182]*

48

reduce ballast degradation. The USP stiffness per unit area ranges from less than 0.10 N/mm^3 up to 0.35 N/mm^3. USP are typically applied in S&C, transition zones and tight curves [185]. Soft USP (0.10 N/mm^3 to 0.25 N/mm^3) have been shown to reduce vibration in the ballast layer [180]. The USP influences the dynamic train-track interaction mainly in the frequency range up to 250 Hz [186]. The implementation of USP has been shown to increase the sleeper–ballast contact area and reduce ballast breakage and abrasion beneath the sleepers [57]. For S&C, Markine et al. [187] and Wan et al. [184] concluded that the use of soft rail pads and USP can significantly reduce the dynamic forces acting on the rails, sleepers and ballast and allow for a smoother transition in vertical track stiffness. Similar results are found in **Paper D**. However, Bruni et al. [37] reported that a turnout installed with soft USP and UBM generated high noise levels. In Switzerland [188] and the UK [41], it was also found that the implementation of soft USPs generates higher acceleration in rail and sleepers. The degradation of track geometry appears to slow down when USPs are used.

UBM is an another elastic element installed below the ballast layer to attenuate vibrations, reduce particle breakage and reduce track stiffness. UBM moduli range from 0.05 to 0.22 N/mm^3 with a thickness of 15 – 30 mm [180]. Typical applications of UBM are on bridges or in tunnels, but its effect becomes limited when the subgrade is soft [180]. Studies have shown that too soft UBM can lead to a decrease in the bearing capacity of the substructure, causing higher dynamic displacements of ballast particles and a higher level of settlement.

For high-speed and high axle load lines, a geogrid is included to provide reinforcement of the ballast [180]. It increases the ballast confinement and lateral resistance, avoids ballast frictional degradation, allows for reducing ballast and sub-ballast thickness without decreasing the bearing capacity of the track [189], and keeps the ballast layer clean by acting as a filter between layers [190]. Its effects have been reviewed by Indraratna et al [11].

From a track superstructure perspective, remedies for reducing high dynamic impact loads have been proposed by Stichel [69]: (1) reduced sleeper spacing, (2) increased effective sleeper base area, (3) increased rail moment of inertia, and (4) use of more resilient (low stiffness) rail pads. Namura & Suzuki [191] suggested that the installation of low-stiffness rail pads on slab track and resilient sleepers with a larger base area on the ballasted track are effective measures to reduce initial ballast settlement and sleeper–ballast contact pressure. The effect of increasing the effective sleeper base area in the crossing panel has also been investigated in **Paper D**. It is found that increasing the sleeper base width and implementation of USP are two efficient measures to reduce the maximum sleeper–ballast contact pressure. However, a larger sleeper base area also increases sleeper mass and crossing panel stiffness, resulting in a less smooth stiffness variation in the crossing panel.

10 Summary of appended papers

In this chapter, a brief summary of the appended papers is presented. Overviews of the studied topics and implemented models are shown in Table 10.1 and Table 10.2.

Table 10.1: Overview of studied topics in the appended papers

Paper	A	B	C	D
Dynamic vehicle–track interaction	✓		✓	✓
Differential track settlement	✓	✓		✓
Iterative scheme	✓			
Mitigation measures				✓

Table 10.2: Overview of implemented models in the appended papers

Paper	A	B	C	D
Track model	moving track model	FE (continuum)	FE (beams,springs) Green's function	FE (beams, springs) Green's function
Vehicle model	whole car	whole car	rigid wheel Green's function	flexible wheelset Green's function
Contact model	multi-Hertz	FE sleeper–ballast	Kalker	Kalker
Settlement model	empirical	constitutive shakedown (CDM)		
Parameter study			train speed rail pad wheel profile lateral wheel position	rail pad sleeper area USP

10.1 Paper A: Simulation of track settlement in railway turnouts

A methodology for the simulation of track settlement in railway turnouts is presented. The methodology predicts the accumulated settlement for a given set of traffic loads using an iterative and cross-disciplinary procedure. The different modules of the procedure include: (I) simulation of dynamic vehicle–track interaction in a turnout applying a validated software for multibody vehicle dynamics considering space-variant track properties, (II) calculation of load distribution and sleeper–ballast contact pressure using a detailed finite element model of a turnout that includes all of the rails (stock rails, switch rails, closure rails, crossing nose, wing rails and check rails), rail pads, baseplates and sleepers on ballast, (III) prediction of track settlement for a given number of load cycles, and (IV) calculation of accumulated track settlement at each sleeper and the resulting vertical track irregularity along the turnout which is used as input in the next step of the iteration. The iteration scheme is demonstrated by calculating the track settlement at the crossing when the studied turnout is exposed to freight traffic in the facing move of the through route.

10.2 Paper B: Three-dimensional modelling of differential railway track settlement using a cycle domain constitutive model

To improve the understanding of the track settlement mechanism in **Paper A**, a method for the simulation of long-term railway track settlement in a crossing panel due to a large number of axle passages is presented. A key ingredient of the method is the cycle domain constitutive model (CDM) proposed by Suiker & de Borst [156], which is used to determine the accumulated (permanent) deformation of the granular layers supporting the railway track. The constitutive model is adopted for both the ballast and the sub-ballast, but with different parameter sets. In this paper, the CDM is used in a three-dimensional finite element representation of a crossing panel subjected to dynamic wheel–rail impact loads, induced by the transfer of wheels between wing rail and crossing nose. Due to the design of the crossing panel and the transient character of the impact load, the load transferred into the track bed is not uniform along the track and the resulting spatially varying (differential) settlement leads to vertical irregularities in track geometry. The spatial variation of track settlement is calculated both along the sleepers and along the rails. The influences of the number of adjacent sleepers accounted for in the model and the stiffness of the subgrade on the predicted settlement are studied.

10.3 Paper C: Simulation of vertical dynamic vehicle–track interaction in a railway crossing using Green's functions

Motivated by the high-frequency contents of the wheel–rail impact load at the crossing, and the need for an accurate prediction of the wheel transition in the crossing panel, the simplified dynamic vehicle–turnout interacton model used in **Paper A** is replaced with an alternative simulation method. The method is based on a moving Green's function approach for the track in combination with an implementation of Kalker's variational method to solve the non-Hertzian, and potentially multiple, wheel–rail contact. The track model is a linear, three-dimensional finite element model of a railway turnout accounting for the variations in rail cross-sections and sleeper lengths, and including baseplates and resilient elements. To deal with the complexity of the track model, involving a large number of elements and degrees-of-freedom, a complex-valued modal superposition with a truncated mode set is applied before the impulse response functions are calculated at various positions along the crossing panel. The variation in three-dimensional contact geometry of the crossing rail and wheel is described by linear surface elements. In each time step of the contact detection algorithm, the lateral position of the wheelset centre is prescribed but the contact positions on wheel and rail are not, allowing for an accurate prediction of the wheel transition between wing rail and crossing rail. The method is demonstrated by calculating the wheel–rail impact load and contact stress distribution for a nominal S1002 wheel profile passing over a nominal crossing geometry. A parameter study is performed to determine the influence of vehicle speed, rail pad stiffness, lateral wheelset position and wheel profile on the impact load generated at the crossing. It is shown that the magnitude of the impact load is influenced more by the wheel–rail contact geometry than by the selection of rail pad stiffness.

10.4 Paper D: Simulation of wheel–rail impact load and sleeper–ballast contact pressure in railway crossings using a Green's function approach

The time-domain vehicle–turnout interaction model presented in **Paper C** is extended to account for both wheels of the wheelset in simultaneous contact with the crossing rail and outer rail. An assessment of mitigation measures to improve the design of railway crossings and reduce the risk of differential settlement is presented. Rigid and flexible wheelset models are compared. The sampled contact geometry of the crossing, including the discrete irregularity between the wing rail and the crossing nose, is used to achieve a three-dimensional surface geometry between each pair of adjacent rail cross-sections. A parameter study is performed to investigate the influence of crossing design on the maximum vertical wheel–rail contact force and the contact pressure generated at the sleeper–ballast interface. It is concluded that a design with a combination of increased sleeper width, softer rail pads and implementation of under sleeper pads (USP) will reduce the track stiffness gradients in the crossing panel and mitigate the risk of differential track settlement by reducing the sleeper–ballast contact pressure.

11 Conclusions and future work

In this chapter, the main achievements of the appended papers are summarised and suggestions for future work are presented. In general, the current work is contributing to the development of improved simulation methodologies to facilitate the prediction of track settlement in railway turnouts.

The contributions include:

- An iterative procedure, combining the strengths of several cross-disciplinary models, to predict accumulated track settlement for a large number of load cycles at any location along the track (**Paper A**)

- A three-dimensional implementation of a cycle-domain constitutive model for ballast, sub-ballast and subgrade accounting for space-variant track characteristics and loading conditions (**Paper B**)

- The prediction of spatial variation of sleeper–ballast contact pressure, both along the sleepers and along the rails (**Papers A, D**)

- The implementation of a method to map the wheel–rail contact force from a time-domain simulation of dynamic vehicle–track interaction to a finite element model of the track that includes a cycle-domain constitutive model (**Paper B**)

- The application of a Green's function approach in a time-domain vehicle–track interaction model, in combination with an implementation of Kalker's variational method to solve the non-Hertzian, and potentially multiple, wheel–rail contact in a railway crossing (**Paper C**)

- A presentation of parameter studies to determine the influence of vehicle speed, rail pad stiffness, lateral wheelset position and wheel profile on the wheel–rail impact load generated at the crossing (**Paper C**)

- The inclusion of a flexible wheelset model in the model for simulation of vehicle–turnout interaction (**Paper D**)

- An assessment of mitigation measures to improve the design of railway crossings with respect to track stiffness, wheel–rail impact load and spatially varying sleeper–ballast contact pressure (**Paper D**)

Some of the major findings include:

- The magnitude of the impact load at a railway crossing is influenced more by the wheel–rail contact geometry than by the selection of rail pad stiffness (**Paper C**)

- The implementation of USP and/or reducing the rail pad stiffness will result in a reduced variation in static track stiffness along the crossing panel, whereas an increase of sleeper base area will increase the stiffness variation (**Paper D**)

- Reducing the rail pad stiffness (from the already low value often used in modern railway crossings) and implementing USP leads to a moderate reduction of the maximum wheel–rail impact load at the crossing (**Paper D**)

- The most effective mitigation measures to reduce sleeper–ballast contact pressure in the crossing panel are the implementation of USP and increasing the sleeper base area (**Paper D**)

- No significant relation between sleeper–ballast contact pressure and rail pad stiffness could be observed (**Paper D**)

Future work:

- The dynamic vehicle–track interaction models presented in this thesis are restricted to linear models (**Papers A, C** and **D**). This means that a tensional load will appear in case the sleeper is lifted from the ballast, and unsupported sleepers due to settlement cannot be accounted for. In future work, nonlinear force-displacement characteristics to represent the conditions in the sleeper–ballast interface should be accounted for. The influence of the simulated densification of the track substructure on the change in track stiffness after each iteration could also be accounted for.

- For the constitutive model of the track substructure, **Paper B** shows that the subgrade model can have a large influence on the stress-strain distribution of the track structure. A softer subgrade leads to reduced deformation of the ballast and sub-ballast layers, but a higher total deformation of the entire substructure. This may call for the need of a refined subgrade model in future work.

- To improve the prediction of long-term accumulated settlement and track degradation using the iterative methodology presented in **Paper A**, the constitutive model in **Paper B** and the vehicle–track interaction method presented in **Paper C** and **Paper D** can be combined.

- The method for simulation of dynamic vehicle–track interaction presented in **Paper C** and **Paper D** is versatile and computationally efficient as long as train speed and the dynamic properties of the track are kept constant. A parameter study aiming towards a minimisation of wheel–rail impact loads and sleeper–ballast contact pressure by optimisation of the rail profiles in the crossing panel can be performed without altering the track model. The design variables could include the crossing nose and wing rail designs, Further, the influence of wear, plastic deformation and RCF of wheel and rail profiles, as well as the wheelset lateral position at the entrance of the crossing panel, can be further investigated using this model.

- Part of the models applied in this thesis have been verified versus field measurements. A further validation by field tests to confirm and demonstrate the conclusions presented in this thesis would be valuable. For example, with the development of measurement technology and condition monitoring, long-term measurements of loads, accelerations and accumulated track settlement can be carried out and used for further model validation.

References

[1] J. H. Sällström, T. Dahlberg, M. Ekh, and J. C. O. Nielsen. *State-of-the-art study on railway turnouts: Dynamics and damage.* Tech. rep. 2004-08. Gothenburg, Sweden: Department of Applied Mechanics, Chalmers University of Technology, 2004. 52 pp.

[2] A. Nissen. "Development of life cycle cost model and analyses for railway switches and crossings". PhD thesis. Luleå, Sweden: Division of Operation, Maintenance Engineering, Department of Civil, Mining, and Environmental Engineering, Luleå University of Technology, 2009.

[3] Trafikverket. *Trafikverkets årsredovisning, annual report.* 2018.

[4] B. A. Pålsson. "Optimisation of railway switches and crossings". PhD thesis. Gothenburg, Sweden: Department of Applied Mechanics, Chalmers University of Technology, 2014.

[5] *Railway applications – Track – Switches and crossings – Part 1: Definitions. EN 13232-1 : 2003.* European committee for standardization. 2003.

[6] E. Kassa. "Dynamic train–turnout interaction: Mathematical modelling, numerical simulation and field testing". PhD thesis. Gothenburg, Sweden: Department of Applied Mechanics, Chalmers University of Technology, 2007.

[7] E. T. Selig and J. M. Waters. *Track geotechnology and substructure management.* T. Telford, 1994.

[8] A. T. Peplow, J. Oscarsson, and T. Dahlberg. *Review of research on ballast as track substructure.* Department of Solid Mechanics/CHARMEC, Chalmers University of Technology: Gothenburg, Sweden, 1996.

[9] G. P. Raymond. Railroad ballast prescription: State-of-the-art. *Journal of the Geotechnical Engineering Division* **105**.2 (1979), 305–322.

[10] J. Y. Zhu. On the effect of varying stiffness under the switch rail on the wheel–rail dynamic characteristics of a high-speed turnout. *Proceedings of the Institution of Mechanical Engineers, Part F: Journal of Rail and Rapid Transit* **220**.1 (2006), 69–75.

[11] B. Indraratna, S. Nimbalkar, and C. Rujikiatkamjorn. A critical review of rail track geotechnologies considering increased speeds and axle loads. *Geotechnical Engineering* **47**.4 (2016), 50–60.

[12] D. Li and E. T. Selig. Cumulative plastic deformation for fine-grained subgrade soils. *Journal of Geotechnical Engineering* **122** (1996), 1006–1013.

[13] G. Lazorenko, A. Kasprzhitskii, Z. Khakiev, and V. Yavna. Dynamic behavior and stability of soil foundation in heavy haul railway tracks: A review. *Construction and Building Materials* **205** (2019), 111–136.

[14] D. Wang, M. Sánchez, and B. J. Behavior of railroads on shrink-swell soils. *E3S Web of Conferences* **9**.20007 (2016).

[15] T Dahlberg. Some railroad settlement models – A critical review. *Proceedings of the Institution of Mechanical Engineers, Part F: Journal of Rail and Rapid Transit* **215**.4 (2001), 289–300.

[16] Y. Sato. Japanese studies on deterioration of ballasted track. *Vehicle System Dynamics* **24**.sup1 (1995), 197–208.

[17] J. E. Alva-Hurtado and E. T. Selig. Permanent strain behaviour of railroad ballast. *Proceedings of the International Conference on Soil Mechanics and Foundation Engineering* **1** (1981), 543–546.

[18] M. J. Shenton. Ballast deformation and track deterioration. *Track Technology* (1985), 253–265.

[19] J. C. O. Nielsen, E. G. Berggren, A. Hammar, F. Jansson, and R. Bolmsvik. Degradation of railway track geometry – Correlation between track stiffness gradient and differential settlement. *Accepted for publication in Proceedings of the Institution of Mechanical Engineers, Part F: Journal of Rail and Rapid Transit* (2020).

[20] E. Andersson, M. Berg, and S. Stichel. *Rail vehicle dynamics*. Division of Rail Vehicles, Department of Aeronautical & Vehicle Eng., Kungliga Tekniska högskolan (KTH): Stockholm, Sweden, 2007.

[21] *Railway applications – Track – Track geometry quality – Part 5: Geometric quality levels – plain line. EN 13848-5 : 2008+A1:2010*. European committee for standardization. 2010. 22 pp.

[22] *Railway applications – Track – Track geometry quality – Part 6: Characterisation of track geometry quality. prEN 13848-6 : 22012*. European committee for standardization. 2012. 26 pp.

[23] R. D. Fröhling. Low frequency dynamic vehicle/track interaction, instrumentation and measurement. *Vehicle System Dynamics* **29** (1998), 1–12.

[24] E. T. Selig and D. Li. Track modulus: Its meaning and factors influencing it. *Transportation Research Record* 1470 (1994), 47–54.

[25] T. Dahlberg. Railway track stiffness variations – Consequences and countermeasures. *International Journal of Civil Eningeering* **8**.1 (2010), 1–12.

[26] W. Powrie and L. Le Pen. *A guide to track stiffness*. University of Southampton, 2016, pp. 1–53.

[27] E. Kabo, J. C. O. Nielsen, and A. Ekberg. Prediction of dynamic train–track interaction and subsequent material deterioration in the presence of insulated rail joints. *Vehicle System Dynamics* **44** (2006), 718–729.

[28] D. Li and D. Davis. Transition of railroad bridge approaches. *Journal of Geotechnical and Geoenvironmental Engineering* **131**.11 (2005), 1392–1398.

[29] B. Coelho, P. Hölscher, J. Priest, W. Powrie, and F. Barends. An assessment of transition zone performance. *Proceedings of the Institution of Mechanical Engineers, Part F: Journal of Rail and Rapid Transit* **225**.2 (2011), 129–139.

[30] H. Wang, V. L. Markine, and X. Liu. Experimental analysis of railway track settlement in transition zones. *Proceedings of the Institution of Mechanical Engineers, Part F: Journal of Rail and Rapid Transit* **232**.6 (2018), 1774–1789.

[31] S. Augustin and G. Gudehus. "Numerical model and laboratory tests on settlement of ballast track". *In Popp, K. and Schiehlen, W. (Eds), System dynamics and long-term behaviour of railway vehicles, track and subgrade.* Springer-Verlag Berlin Heidelberg, 2003, pp. 317–336.

[32] Y. Bezin, S. D. Iwnicki, M. Cavalletti, E. De Vries, F. Shahzad, and G. Evans. An investigation of sleeper voids using a flexible track model integrated with railway multi-body dynamics. *Proceedings of the Institution of Mechanical Engineers, Part F: Journal of Rail and Rapid Transit* **223**.6 (2009), 597–607.

[33] J. Zhang, C. Wu, X. Xiao, Z. Wen, and X. Jin. Effect of unsupported sleepers on sleeper dynamic response. *Xinan Jiaotong Daxue Xuebao/Journal of Southwest Jiaotong University* **45**.2 (2010), 203–208.

[34] J. C. O. Nielsen and X. Li. Railway track geometry degradation due to differential settlement of ballast/subgrade Numerical prediction by an iterative procedure. *Journal of Sound and Vibration* **412** (2018), 441–456.

[35] E. Berggren. "Railway track stiffness – Dynamic measurements and evaluation for efficient maintenance". PhD thesis. Stockholm, Sweden: Division of Rail Vehicles, Department of Aeronautical and Vehicle Engineering, Royal Institute of Technology (KTH), 2009.

[36] TURNOUTS. *New concepts for turnouts in urban rail transit infrastructures.* No. FP-6-505592. TURNOUTS Project, 2007. 78 pp.

[37] S. Bruni, I. Anastasopoulos, S. Alfi, A. V. Leuven, and G. Gazetas. Effects of train impacts on urban turnouts: Modelling and validation through measurements. *Journal of Sound and Vibration* **324**.3 (2009), 666–689.

[38] C. Wan, V. L. Markine, and I. Y. Shevtsov. Improvement of vehicle–turnout interaction by optimising the shape of crossing nose. *Vehicle System Dynamics* **52**.11 (2014), 1517–1540.

[39] A. Paixão, C. Alves Ribeiro, N. Pinto, E. Fortunato, and R. Calcada. On the use of under sleeper pads in transition zones at railway underpasses: Experimental field testing. *Structure and Infrastructure Engineering* **11**.2 (2015), 112–128.

[40] L. Le Pen, G. Watson, W. Powrie, G. Yeo, P. Weston, and C. Roberts. The behaviour of railway level crossings: Insights through field monitoring. *Transportation Geotechnics* **1**.4 (2014), 201–213.

[41] L. Le Pen, G. Watson, A. Hudson, and W. Powrie. Behaviour of under sleeper pads at switches and crossings Field measurements. *Proceedings of the Institution*

of Mechanical Engineers, Part F: Journal of Rail and Rapid Transit **232**.4 (2018), 1049–1063.

[42]   J. Jönsson, I. Arasteh khouy, J. Lundberg, M. Rantatalo, and A. Nissen. Measurement of vertical geometry variations in railway turnouts exposed to different operating conditions. *Proceedings of the Institution of Mechanical Engineers, Part F: Journal of Rail and Rapid Transit* **230**.2 (2015).

[43]   J. Oscarsson. "Dynamic train–track interaction: linear and non-linear track models with property scatter". PhD thesis. Gothenburg, Sweden: Department of Solid Mechanics, Chalmers University of Technology, 2001.

[44]   L. Le Pen, D. Milne, G. Watson, J. Harkness, and W. Powrie. A model for the stochastic prediction of track support stiffness. *Proceedings of the Institution of Mechanical Engineers, Part F: Journal of Rail and Rapid Transit* (2019).

[45]   E. G. Berggren, A. Nissen, and B. S. Paulsson. Track deflection and stiffness measurements from a track recording car. *Proceedings of the Institution of Mechanical Engineers, Part F: Journal of Rail and Rapid Transit* **228**.6 (2014), 570–580.

[46]   E. Kassa and J. C. O. Nielsen. Dynamic interaction between train and railway turnout: Full-scale field test and validation of simulation models. *Vehicle System Dynamics* **46** (2008), 521–534.

[47]   B. A. Pålsson and J. C. O. Nielsen. Dynamic vehicle–track interaction in switches and crossings and the influence of rail pad stiffness – Field measurements and validation of a simulation model. *Vehicle System Dynamics* **53**.6 (2015), 734–755.

[48]   INNOTRACK. *Methods of track stiffness measurements.* INNOTRACK project No. TIP5-CT-2006-031415. 2006. 36 pp.

[49]   INNOTRACK. *Concluding technical report.* Tech. rep. International Union of Railways (UIC), Paris, France, 2010. 288 pp.

[50]   R. Bolmsvik, J. C. O. Nielsen, P. Kron, and B. A. Pålsson. *Switch sleeper specification.* Tech. rep. 2010-03. Gothenburg, Sweden: Department of Applied Mechanics, Chalmers University of Technology, 2010. 54 pp.

[51]   I. Arasteh Khouy, P.-O. Larsson-Kråik, A. Nissen, J. Lundberg, and U. Kumar. Geometrical degradation of railway turnouts: A case study from a Swedish heavy haul railroad. *Proceedings of the Institution of Mechanical Engineers, Part F: Journal of Rail and Rapid Transit* **228**.6 (2014), 611–619.

[52]   G. P. Raymond and D. R. Williams. Repeated load triaxial tests on a dolomite ballast. *Journal of the Geotechnical Engineering Division* **104**.7 (1978), 1013–1029.

[53]   A. S. J. Suiker, E. T. Selig, and R. Frenkel. Static and cyclic triaxial testing of ballast and subballast. *Journal of Geotechnical and Geoenvironmental Engineering* **131**.6 (2005), 771–782.

[54] B. Indraratna, D. Ionescu, and H. D. Christie. Shear behavior of railway ballast based on large-scale triaxial tests. *Journal of Geotechnical and Geoenvironmental Engineering* **124**.5 (1998), 439–449.

[55] J. Lackenby, B. Indraratna, G. McDowell, and D. Christie. Effect of confining pressure on ballast degradation and deformation under cyclic triaxial loading. *Geotechnique* **57**.6 (2007), 527–536.

[56] B. Indraratna, N. Ngo, C. Rujikiatkamjorn, and J. Vinod. Behavior of fresh and fouled railway ballast subjected to direct shear testing: Discrete element simulation. *International Journal of Geomechanics* **14**.1 (2014), 34–44.

[57] H. Li and G. McDowell. Discrete element modelling of under sleeper pads using a box test. *Granular Matter* **20**.2 (2018).

[58] J. Dijkstra and W. Broere. New method of full-field stress analysis and measurement using photoelasticity. *Geotechnical Testing Journal* **33**.6 (2010).

[59] S. Stanier, J. Dijkstra, D. Leniewska, J. Hambleton, D. White, and D. Muir Wood. Vermiculate artefacts in image analysis of granular materials. *Computers and Geotechnics* **72** (2016), 100–113.

[60] F. Lekarp and A. Dawson. Modelling permanent deformation behaviour of unbound granular materials. *Construction and Building Materials* **12**.1 (1998), 9–18.

[61] S. Werkmeister, A. R. Dawson, and F. Wellner. Permanent deformation behavior of granular materials and the shakedown concept. *Transportation Research Record* 1757 (2001), 75–81.

[62] R. Garcia-Rojo and H. J. Herrmann. Shakedown of unbound granular material. *Granular Matter* **7**.2–3 (2005), 109–118.

[63] Q. D. Sun, B. Indraratna, and S. Nimbalkar. Effect of cyclic loading frequency on the permanent deformation and degradation of railway ballast. *Geotechnique* **64**.9 (2014), 746–751.

[64] M. Baessler and W. Ruecker. "Track settlement due to cyclic loading with low minimum pressure and vibrations". *In Popp, K. and Schiehlen, W. (Eds), System dynamics and long-term behaviour of railway vehicles, track and subgrade.* Springer-Verlag Berlin Heidelberg, 2003, pp. 337–356.

[65] T. Abadi, L. Le Pen, A. Zervos, and W. Powrie. Improving the performance of railway tracks through ballast interventions. *Proceedings of the Institution of Mechanical Engineers, Part F: Journal of Rail and Rapid Transit* **232**.2 (2018), 337–355.

[66] V. Cuellar, J. Estaire, F. Navarro, M. A. Andreu, M. Rodriguez, A. Andres, W. Rucker, E. Bongini, A. Pieringer, R. Garburg, F. Baldrick, E. Knothe, S. Schwieger, L. Auersch, and H. Flöttmann. *RIVAS report D 3.7 (SCP0-GA-2010-265754): Results of laboratory tests for ballasted track mitigation measures CEDEX*

track box tests. RIVAS report D 3.7 (SCP0-GA-2010-265754). RIVAS Project, 2013. 4 pp.

[67] A. S. Suiker. "The mechanical behaviour of ballasted railway tracks". PhD thesis. The Netherlands: Department of Civil Engineering and Geosciences, Delft University of Technology, 2002.

[68] S. D. Iwnicki, S. L. Grassie, and W. Kik. Track settlement prediction using computer simulation tools. *Vehicle System Dynamics* **33** (2000), 2–12.

[69] S. Stichel. On freight wagon dynamics and track deterioration. *Proceedings of the Institution of Mechanical Engineers, Part F: Journal of Rail and Rapid Transit* **213**.4 (1999), 243–254.

[70] M. Ishida and T. Suzuki. *Quarterly Report of RTRI (Railway Technical Research Institute, Japan)* **46**.1 (2005), 1–6.

[71] L. A. Yang, W. Powrie, and J. A. Priest. Dynamic stress analysis of a ballasted railway track bed during train passage. *Journal of Geotechnical and Geoenvironmental Engineering* **135**.5 (2009), 680–689.

[72] Y. Bezin, I. Grossoni, and S. Neves. "Impact of wheel shape on the vertical damage of cast crossing panels in turnouts". 2016, pp. 1163–1172.

[73] J. C. O. Nielsen and A. Johansson. Out-of-round railway wheels – A literature survey. *Proceedings of the Institution of Mechanical Engineers, Part F: Journal of Rail and Rapid Transit* **214**.2 (2000), 79–91.

[74] A. Johansson and J. C. O. Nielsen. Out-of-round railway wheels – Wheel–rail contact forces and track response derived from field tests and numerical simulations. *Proceedings of the Institution of Mechanical Engineers, Part F: Journal of Rail and Rapid Transit* **217**.2 (2003), 135–145.

[75] K. Knothe and S. L. Grassie. Modelling of railway track and vehicle/track interaction at high frequencies. *Vehicle System Dynamics* **22**.3–4 (1993), 209–262.

[76] K. Popp, K. Knothe, and C. Pöpper. System dynamics and long-term behaviour of railway vehicles, track and subgrade: Report on the DFG Priority Programme in Germany and subsequent research. *Vehicle System Dynamics* **43**.6–7 (2005), 485–521.

[77] R. D. Cook, D. S. Malkus, and M. E. Plesha. *Concepts and applications of finite element analysis*. 4th ed. John Wiley & Sons, Inc, 2002. 719 pp.

[78] ABAQUS. *Users' Manual*. Dassault Systémes. 2013.

[79] R. Andersson. "Squat defects and rolling contact fatigue clusters – Numerical investigations of rail and wheel deterioration mechanisms ". PhD thesis. Gothenburg, Sweden: Department of Applied Mechanics, Chalmers University of Technology, 2017.

[80] R. R. Craig and A. J. Kurdila. *Foundamentals of Structural Dynamics*. 2nd ed. John Wiley & Sons, Inc, 2006. 728 pp.

[81] A. Pieringer. "Time-domain modelling of high-frequency wheel/rail interaction". PhD thesis. Gothenburg, Sweden: Division of Applied Acoustics, Vibroacoustic Group, Department of Civil and Environmental Engineering, Chalmers University of Technology, 2011.

[82] A. Nordborg. Wheel/rail noise generation due to nonlinear effects and parametric excitation. *The Journal of the Acoustical Society of America* **111**.4 (2002), 1772–1781.

[83] T. Mazilu. Green's functions for analysis of dynamic response of wheel/rail to vertical excitation. *Journal of Sound and Vibration* **306**.1–2 (2007), 31–58.

[84] T. Mazilu, M. Dumitriu, and C. Tudorache. On the dynamics of interaction between a moving mass and an infinite one-dimensional elastic structure at the stability limit. *Journal of Sound and Vibration* **330**.15 (2011), 3729–3743.

[85] T. Mazilu. Instability of a train of oscillators moving along a beam on a viscoelastic foundation. *Journal of Sound and Vibration* **332**.19 (2013), 4597–4619.

[86] I. Zenzerovic, W. Kropp, and A. Pieringer. An engineering time-domain model for curve squeal: Tangential point-contact model and Green's functions approach. *Journal of Sound and Vibration* **376** (2016), 149–165.

[87] P. T. Torstensson, G. Squicciarini, M. Krüger, J. C. O. Nielsen, and D. J. Thompson. "Hybrid model for prediction of impact noise generated at railway crossings". *Noise and Vibration Mitigation for Rail Transportation Systems*. Cham: Springer International Publishing, 2018, pp. 759–769.

[88] T. J. S. Abrahamsson. "Modal analysis and synthesis in transient vibration and structural optimization problems". PhD thesis. Gothenburg, Sweden: Department of Solid Mechanics, Chalmers University of Technology, 1990.

[89] J. C. O. Nielsen and T. J. S. Abrahamsson. Coupling of physical and modal components for analysis of moving nonlinear dynamic systems on general beam structures. *International Journal for Numerical Methods in Engineering* **33**.9 (1992), 1843–1859.

[90] P. T. Torstensson. "Rail Corrugation Growth on Curves". PhD thesis. Gothenburg, Sweden: Department of Applied Mechanics, Chalmers University of Technology, 2012.

[91] J. C. O. Nielsen and J. Oscarsson. Simulation of dynamic train–track interaction with state-dependent track properties. *Journal of Sound and Vibration* **275**.3–5 (2004), 515–532.

[92] GENSYS. *Release 100903*. AB DEsolver. Östersund, Sweden, 2010.

[93] C. Wan, V. L. Markine, and I. Y. Shevtsov. Analysis of train/turnout vertical interaction using a fast numerical model and validation of that model. *Proceedings of the Institution of Mechanical Engineers, Part F: Journal of Rail and Rapid Transit* **228**.7 (2014), 730–743.

[94] C. Wan, V. L. Markine, and I. Shevtsov. Optimisation of the elastic track properties of turnout crossings. *Proceedings of the Institution of Mechanical Engineers, Part F: Journal of Rail and Rapid Transit* **230**.2 (2016), 360–373.

[95] T. Suzuki, M. Ishida, K. Abe, and K. Koro. Measurement on dynamic behaviour of track near rail joints and prediction of track settlement. *Quarterly Report of RTRI (Railway Technical Research Institute, Japan)* **46** (2 2005), 124–129.

[96] I. Grossoni, S. D. Iwnicki, Y. Bezin, and C. Gong. Dynamics of a vehicle–track coupling system at a rail joint. *Proceedings of the Institution of Mechanical Engineers, Part F: Journal of Rail and Rapid Transit* **229**.4 (2015), 364–374.

[97] J. C. O. Nielsen and A. Igeland. Vertical dynamic interaction between train and track – Influence of wheel and track imperfections. *Journal of Sound and Vibration* **187**.5 (1995), 825–839.

[98] E. Kassa, C. Andersson, and J. C. O. Nielsen. Simulation of dynamic interaction between train and railway turnout. *Vehicle System Dynamics* **44**.3 (2006), 247–258.

[99] I. Grossoni, Y. Bezin, and S. Neves. Optimisation of support stiffness at railway crossings. *Vehicle System Dynamics* **56**.7 (2018), 1072–1096.

[100] W. Zhai and X. Sun. A detailed model for investigating vertical interaction between railway vehicle and track. *Vehicle System Dynamics* **23** (1994), 603–615.

[101] Y. Sun, Y. Guo, Z. Chen, and W. Zhai. Effect of differential ballast settlement on dynamic response of vehicle–track coupled systems. *International Journal of Structural Stability and Dynamics* **18**.7 (2018).

[102] Y. Guo and W. Zhai. Long-term prediction of track geometry degradation in high-speed vehcile ballastless track system due to differential subgrade settlement. *Publication under process* (2019).

[103] W. Zhai, Z. Han, Z. Chen, L. Ling, and S. Zhu. Train–track–bridge dynamic interaction: A state-of-the-art review. *Vehicle System Dynamics* **57**.7 (2019), 984–1027.

[104] J. C. O. Nielsen, B. A. Pålsson, and P. T. Torstensson. Switch panel design based on simulation of accumulated rail damage in a railway turnout. *Wear* **366–367** (2016), 241–248.

[105] C. Andersson and T. Dahlberg. Wheel/rail impacts at a railway turnout crossing. *Proceedings of the Institution of Mechanical Engineers, Part F: Journal of Rail and Rapid Transit* **212**.2 (1998), 123–134.

[106] S. Alfi and S. Bruni. Mathematical modelling of train–turnout interaction. *Vehicle System Dynamics* **47**.5 (2009), 551–574.

[107] R. R. J. Craig and M. C. C. Bampton. Coupling of substructures for dynamic analyses. *AIAA Journal* **6**.7 (1968), 1313–1319.

[108] B. Pålsson. *Chapter 3.4.3 in Enhanced S&C Whole System Analysis, Design and Virtual Validation*. Report D2.2. In2Track, 2018, pp. 97–107.

[109] A. Lundqvist and T. Dahlberg. Dynamic train/track interaction including model for track settlement evolvement. *Vehicle System Dynamics* **41** (2004), 667–676.

[110] H. Wang and V. L. Markine. Modelling of the long-term behaviour of transition zones: Prediction of track settlement. *Engineering Structures* **156** (2018), 294–304.

[111] J. N. Varandas, P. Hölscher, and M. A. G. Silva. Three-dimensional track–ballast interaction model for the study of a culvert transition. *Soil Dynamics and Earthquake Engineering* **89** (2016), 116–127.

[112] M. Pletz, W. Daves, and H. Ossberger. A wheelset/crossing model regarding impact, sliding and deformation – Explicit finite element approach. *Wear* **294–295** (2012), 446–456.

[113] W. Cai, Z. Wen, X. Jin, and W. Zhai. Dynamic stress analysis of rail joint with height difference defect using finite element method. *Engineering Failure Analysis* **14**.8 (2007), 1488–1499.

[114] L. Xin, V. L. Markine, and I. Y. Shevtsov. Numerical procedure for fatigue life prediction for railway turnout crossings using explicit finite element approach. *Wear* **366–367** (2016), 167–179.

[115] K. Popp, H. Kruse, and I. Kaiser. Vehicle-track dynamics in the mid-frequency range. *Vehicle System Dynamics* **31**.5–6 (1999), 423–464.

[116] M. S. Sichani. "On efficient modelling of wheel–rail contact in vehicle dynamics simulation". PhD thesis. Stockholm, Sweden: Department of Aeronautical and Vehicle Engineering, Royal Institute of Technology (KTH), 2016.

[117] J. A. Elkins. Prediction of wheel/rail interaction: The state-of-the-art. *Vehicle System Dynamics* **20** (1992), 1–27.

[118] J. J. Kalker. A fast algorithm for the simplified theory of rolling-contact. *Vehicle System Dynamics* **11**.1 (1982), 1–13.

[119] H. Hertz. Üeber die Berührung fester elastischer Körper. *Journal für reine und angewandte Mathematik* **92** (1882), 156–171.

[120] K. L. Johnson. *Contact mechanics*. Cambridge Univ. Press: Cambridge, 1985.

[121] R. Skrypnyk, J. C. O. Nielsen, M. Ekh, and B. A. Pålsson. Metamodelling of wheel-rail normal contact in railway crossings with elasto-plastic material behaviour. *Engineering with Computers* **35**.1 (2019), 139–155.

[122] W. Yan and F. D. Fischer. Applicability of the Hertz contact theory to rail-wheel contact problems. *Archive of Applied Mechanics* **70**.4 (2000), 255–268.

[123] M. Wiest, E. Kassa, W. Daves, J. C. O. Nielsen, and H. Ossberger. Assessment of methods for calculating contact pressure in wheel–rail/switch contact. *Wear* **265**.9–10 (2008), 1439–1445.

[124] J. P. Pascal and G. Sauvage. Available methods to calculate the wheel/rail forces in non-Hertzian contact patches and rail damaging. *Vehicle System Dynamics* **22**.3–4 (1993), 263–275.

[125] J. B. Ayasse and H. Chollet. Determination of the wheel–rail contact patch in semi-Hertzian conditions. *Vehicle System Dynamics* **43**.3 (2005), 161–172.

[126] J. Piotrowski and W. Kik. A simplified model of wheel/rail contact mechanics for non-Hertzian problems and its application in rail vehicle dynamics. *Vehicle System Dynamics* **46**.1–2 (2008), 27–48.

[127] J. J. Kalker. Contact mechanical algorithms. *Communications in Applied Numerical Methods* **4**.1 (1988), 25–32.

[128] E. A. H. Vollebregt. *User guide for CONTACT, Vollebregt and Kalker's rolling and sliding contact model*. Tech. rep. TR09-03, version 13.1. VORTech, Delft, The Netherlands, 2012. 54 pp.

[129] E. A. H. Vollebregt. Numerical modeling of measured railway creep versus creep-force curves with CONTACT. *Wear* **314**.1–2 (2014), 87–95.

[130] J. Zhao, E. A. H. Vollebregt, and C. W. Oosterlee. Extending the BEM for elastic contact problems beyond the half-space approach. *Mathematical Modelling and Analysis* **21**.1 (2016), 119–141.

[131] E. A. H. Vollebregt. Conformal contact: Corrections and new results. *Vehicle System Dynamics* **56**.10 (2018), 1622–1632.

[132] A. Draganis. "Numerical simulation of thermomechanically coupled transient rolling contact – An arbitrary Lagrangian-Eulerian approach ". PhD thesis. Gothenburg, Sweden: Department of Applied Mechanics, Chalmers University of Technology, 2014.

[133] D. Li and E. T. Selig. Resilient modulus for fine-grained subgrade soils. *Journal of Geotechnical Engineering* **120**.6 (1994), 939–957.

[134] F. Lekarp, U. Isacsson, and A. Dawson. State of the art. I: Resilient response of unbound aggregates. *Journal of Transportation Engineering* **126**.1 (2000), 66–75.

[135] M. Shenton. Deformation of railway ballast under repeated loading conditions. *Railroad Track Mechanics and Technology* (1978), 405–425.

[136] A. Hettler. Bleibende Setzungen des Schotteroberbaus. *Eisenbahn-technische Rundschau (ETR)* **33**.11 (1984), 847–853.

[137] B. Indraratna, N. Ngo, and C. Rujikiatkamjorn. Deformation of coal fouled ballast stabilized with geogrid under cyclic load. *Journal of Geotechnical and Geoenvironmental Engineering* **139**.8 (2013), 1275–1289.

[138] ORE. *Stresses in the rails, the ballast and in the formation resulting from traffic loads*. D 71/RP 10/E 00052874. International Union of Railways, 1968. 39 pp.

[139] T. Ishikawa, S. Miura, and E. Sekine. Simple plastic deformation analysis of ballasted track under repeated moving-wheel loads by cumulative damage model. *Transportation Geotechnics* **1**.4 (2014), 157–170.

[140] N. Guérin. "Approche expérimental et numérique du comportement du ballast des voies ferrées". PhD thesis. Paris, France: Ecole Nationale des Pont et Chaussées, 1996.

[141] T. Abadi, L. Le Pen, A. Zervos, and W. Powrie. A review and evaluation of ballast settlement models using results from the Southampton Railway Testing Facility (SRTF). *Procedia Engineering* **143** (2016), 999–1006.

[142] I. Grossoni, A. R. Andrade, Y. Bezin, and S. Neves. The role of track stiffness and its spatial variability on long-term track quality deterioration. *Proceedings of the Institution of Mechanical Engineers, Part F: Journal of Rail and Rapid Transit* **233**.1 (2019), 16–32.

[143] Y. Sato. Optimization of track maintenance work on ballasted track. *Proceedings of the World Congress on Railway Research (WCRR '97)* **B** (1997), 405–411.

[144] H. Kruse and K. Popp. "Model-based investigation of the dynamic behaviour of railway ballast". *In Popp, K. and Schiehlen, W. (Eds), System dynamics and long-term behaviour of railway vehicles, track and subgrade.* Springer-Verlag Berlin Heidelberg, 2003, pp. 275–294.

[145] C.-L. Liao, T.-P. Chang, D.-H. Young, and C. S. Chang. Stress strain relationship for granular materials based on the hypothesis of best fit. *International Journal of Solids and Structures* **34**.31–32 (1997), 4087–4100.

[146] C. S. Chang, S. J. Chao, and Y. Chang. Estimates of elastic moduli for granular material with anisotropic random packing structure. *International Journal of Solids and Structures* **32**.14 (1995), 1989–2008.

[147] G. Saussine, C. Cholet, P. E. Gautier, F. Dubois, C. Bohatier, and J. J. Moreau. Modelling ballast behaviour under dynamic loading. Part 1: A 2D polygonal discrete element method approach. *Computer Methods in Applied Mechanics and Engineering* **195** (2006), 2841–2859.

[148] W. L. Lim and G. R. McDowell. Discrete element modelling of railway ballast. *Granular Matter* **7**.1 (2005), 19–29.

[149] S. Lobo-Guerrero, L. E. Vallejo, and L. F. Vesga. Visualization of crushing evolution in granular materials under compression using DEM. *International Journal of Geomechanics* **6**.3 (2006), 195–200.

[150] B. Indraratna, P. K. Thakur, and J. S. Vinod. Experimental and numerical study of railway ballast behaviour under cyclic loading. *International Journal of Geomechanics* **10**.4 (2010), 136–144.

[151] C. Chen, G. R. McDowell, and N. H. Thom. Investigating geogrid-reinforced ballast: Experimental pull-out tests and discrete element modelling. *Soils and Foundations* **54**.1 (2014), 1–11.

[152] A. Karrech, D. Duhamel, G. Bonnet, J. Roux, F. Chevoir, J. Canou, J. C. Dupla, and K. Sab. A computational procedure for the prediction of settlement in granular materials under cyclic loading. *Computer Methods in Applied Mechanics and Engineering* **197**.1–4 (2007), 80–94.

[153] C. Chazallon, P. Hornych, and S. Mouhoubi. Elastoplastic model for the long-term behavior modeling of unbound granular materials in flexible pavements. *International Journal of Geomechanics* **6**.4 (2006), 279–289.

[154] M. Abdelkrim, G. Bonnet, and P. de Buhan. A computational procedure for predicting the long term residual settlement of a platform induced by repeated traffic loading. *Computers and Geotechnics* **30**.6 (2003), 463–476.

[155] F. Lekarp, U. Isacsson, and A. Dawson. State of the art. II: Permanent strain response of unbound aggregates. *Journal of Transportation Engineering* **126**.1 (2000), 76–83.

[156] A. S. J. Suiker and R. de Borst. A numerical model for the cyclic deterioration of railway tracks. *International Journal for Numerical Methods in Engineering* **57**.4 (2003), 441–470.

[157] L. Jacobsson and K. Runesson. "Computational modelling of high-cycle conditioning of railway ballast". *Proceedings of the European Conference on Computational Mechaincs*. Cracow, Poland, 2001.

[158] V. H. Nguyen, D. Duhamel, and B. Nedjar. A continuum model for granular materials taking into account the no-tension effect. *Mechanics of Materials* **35** (2003), 955–967.

[159] P. V. Lade and J. M. Duncan. Elastoplastic stress-strain theory for cohesionless soil. *Journal of the Geotechnical Engineering Division* **101**.10 (1975), 1037–1053.

[160] Z. Mroz, V. A. Norris, and O. C. Zienkiewicz. Anisotropic hardening model for soils and its application to cyclic loading. *International Journal for Numerical and Analytical Methods in Geomechanics* **2**.3 (1978), 203–221.

[161] P. A. Vermeer and R. de Borst. Non-associated plasticity for soils, concrete and rock. *Heron* **29**.3 (1984).

[162] Y. J. Cui and P. Delage. Yielding and plastic behaviour of an unsaturated compacted silt. *Geotechnique* **46**.2 (1996), 291–311.

[163] T. Nakai and M. Hinokio. A simple elastoplastic model for normally and over consolidated soils with unified material parameters. *Soils and Foundations* **44**.2 (2004), 53–70.

[164] Y. P. Yao, D. A. Sun, and H. Matsuoka. A unified constitutive model for both clay and sand with hardening parameter independent on stress path. *Computers and Geotechnics* **35**.2 (2008), 210–222.

[165] P.-A. von Wolffersdorff. Hypoplastic relation for granular materials with a predefined limit state surface. *Mechanics of Cohesive-Frictional Materials* **1**.3 (1996), 251–271.

[166] I. Herle and G. Gudehus. Determination of parameters of a hypoplastic constitutive model from properties of grain assemblies. *Mechanics of Cohesive-Frictional Materials* **4**.5 (1999), 461–486.

[167] Z.-L. Wang, Y. F. Dafalias, and C.-K. Shen. Bounding surface hypoplasticity model for sand. *Journal of Engineering Mechanics* **116**.5 (1990), 983–1001.

[168] B. Indraratna, J. Lackenby, and D. Christie. Effect of confining pressure on the degradation of ballast under cyclic loading. *Geotechnique* **55**.4 (2005), 325–328.

[169] B. Indraratna and W. Salim. Modelling of particle breakage of coarse aggregates incorporating strength and dilatancy. *Proceedings of the Institution of Civil Engineers: Geotechnical Engineering* **155**.4 (2002), 243–252.

[170] B. Indraratna, P. K. Thakur, J. S. Vinod, and W. Salim. Semiempirical cyclic densification model for ballast incorporating particle breakage. *International Journal of Geomechanics* **12**.3 (2012), 260–271.

[171] T. Wichtmann, H. A. Rondón, A. Niemunis, T. Triantafyllidis, and A. Lizcano. Prediction of permanent deformations in pavements using a high-cycle accumulation model. *Journal of Geotechnical and Geoenvironmental Engineering* **136** (2010), 728–740.

[172] R. W. Sharp and J. R. Booker. Shakedown of pavements under moving surface loads. *Journal of Transportation Engineering* **110**.1 (1984), 1–14.

[173] I. F. Collins and M. Boulbibane. Geomechanical analysis of unbound pavements based on shakedown theory. *Journal of Geotechnical and Geoenvironmental Engineering* **126**.1 (2000), 50–59.

[174] C. Chazallon, G. Koval, and S. Mouhoubi. A two-mechanism elastoplastic model for shakedown of unbound granular materials and DEM simulations. *International Journal for Numerical and Analytical Methods in Geomechanics* **36**.17 (2012), 1847–1868.

[175] C. S. Desai. Unified DSC constitutive model for pavement materials with numerical implementation. *International Journal of Geomechanics* **7**.2 (2007), 83–101.

[176] A. Niemunis, T. Wichtmann, and T. Triantafyllidis. A high-cycle accumulation model for sand. *Computers and Geotechnics* **32**.4 (2005), 245–263.

[177] C. Pasten, H. Shin, and J. Carlos Santamarina. Long-term foundation response to repetitive loading. *Journal of Geotechnical and Geoenvironmental Engineering* **140**.4 (2014).

[178] T. Wichtmann, A. Niemunis, and T. Triantafyllidis. Flow rule in a high-cycle accumulation model backed by cyclic test data of 22 sands. *Acta Geotechnica* **9**.4 (2014), 695–709.

[179] J. N. Varandas, P. Hölscher, and M. A. G. Silva. Settlement of ballasted track under traffic loading: Application to transition zones. *Proceedings of the Institution of Mechanical Engineers, Part F: Journal of Rail and Rapid Transit* **228**.3 (2014), 242–259.

[180] M. Sol-Sanchez and G. D'Angelo. Review of the design and maintenance technologies used to decelerate the deterioration of ballasted railway tracks. *Construction and Building Materials* **157** (2017), 402–415.

[181] S. Kaewunruen and A. M. Remennikov. Effect of improper ballast packing/tamping on dynamic behaviors of on-track railway concrete sleeper. *International Journal of Structural Stability and Dynamics* **7**.1 (2007), 167–177.

[182] M. Sol-Sanchez, F. Moreno-Navarro, and M. C. Rubio-Gamez. Analysis of ballast tamping and stone-blowing processes on railway track behaviour: the influence of using USPs. *Géotechnique* **66**.6 (2016), 481–489.

[183] S. Kaewunruen. "Effectiveness of using elastomeric pads to mitigate impact vibration at an urban turnout crossing". *Notes on Numerical Fluid Mechanics and Multidisciplinary Design*. Vol. 118. Springer-Verlag Berlin Heidelberg, 2012, pp. 357–365.

[184] C. Wan, V. L. Markine, and I. Y. Shevtsov. Optimisation of the elastic track properties of turnout crossings. *Proceedings of the Institution of Mechanical Engineers, Part F: Journal of Rail and Rapid Transit* **230**.2 (2016), 360–373.

[185] UIC. *USP recommendations – Under Sleeper Pads, Recommendations for Use*. 2013.

[186] A. Johansson, J. C. O. Nielsen, R. Bolmsvik, A. Karlström, and R. Lundén. Under sleeper pads – Influence on dynamic train–track interaction. *Wear* **265**.9–10 (2008), 1479–1487.

[187] V. L. Markine, M. J. M. M. Steenbergen, and I. Y. Shevtsov. Combatting RCF on switch points by tuning elastic track properties. *Wear* **271**.1–2 (2011), 158–167.

[188] P. Schneider, R. Bolmsvik, and J. C. O. Nielsen. In situ performance of a ballasted railway track with under sleeper pads. *Proceedings of the Institution of Mechanical Engineers, Part F: Journal of Rail and Rapid Transit* **225**.3 (2011), 299–309.

[189] B. Indraratna, W. Salim, and C. Rujikiatkamjorn. *Advanced rail geotechnology – Ballasted track*. 2011. 410 pp.

[190] B. Indraratna, H. Khabbaz, W. Salim, and D. Christie. Geotechnical properties of ballast and the role of geosynthetics in railtrack stabilisation. *Journal of Ground Improvement* **10**.3 (2006), 91–102.

[191] A. Namura and T. Suzuki. Evaluation of countermeasures against differential settlement at track transitions. *Quarterly Report of RTRI (Railway Technical Research Institute, Japan)* **48**.3 (2007), 176–182.

Part II

Appended Papers A–D

Paper A

Simulation of track settlement in railway turnouts

Paper B

Three-dimensional modelling of differential railway track settlement using a cycle domain constitutive model

Paper C

Simulation of vertical dynamic vehicle–track interaction in a railway crossing using Green's functions

Paper D

Simulation of wheel–rail impact load and sleeper–ballast contact pressure in railway crossings using a Green's function approach

A SOLID GROUND FOR THE UNDERSTANDING OF TRACK SETTLEMENT IN RAILWAY CROSSINGS

Railway turnouts (switches and crossings, S&C) are critical components in the railway system. They provide flexibility in traffic routes by allowing trains to switch from one track to another. To serve this purpose, the turnout consists of both movable and fixed mechanical parts, as well as systems for mechatronics and signalling. In Sweden alone, there are about 14 000 S&Cs in the 16 600 km of railway network.

Turnouts stand for significant contributions to the number of reported track faults and the total cost for railway maintenance. In 2018, the cost for maintenance of turnouts in Sweden was MSEK 530, corresponding to about 10 % of the total railway maintenance cost. Further, it was the railway component that caused most train delays. One of the main drivers for the high maintenance costs is the need to repair and replace switch rails and crossings as these components are subjected to a severe load environment resulting in the degradation of rail profiles and track geometry.

One contribution to the degradation of track geometry in turnouts is differential track settlement. This is a phenomenon where the horizontal level of the supporting track substructure decreases in height over time when subjected to repeated traffic loading. Dynamic wheel–rail contact forces with high magnitudes are generated in the switch and crossing panels due to the discontinuities in rail profiles that are necessary to allow for the rerouting of traffic. Because of the turnout design and the variation in track support conditions, the load transferred into the track bed is not uniform, thus resulting in a variation in settlement along the track and irregularities in track geometry. Poor quality in track geometry induces higher dynamic wheel–rail contact forces that further increase the degradation of rail profiles and track geometry.

The present work aims to provide a methodology to improve the understanding of differential track settlement in railway turnouts. This includes predictions of the high-magnitude wheel–rail impact loads on the crossing generated by passing trains with worn wheel profiles, the distribution of contact pressure between sleepers and ballast, and the accumulated permanent deformation of the track substructure.

Another objective is to provide an accurate and generic simulation environment accounting for the multiple wheel–rail contacts in the crossing panel and considering the high-frequency dynamic interaction between the vehicle and the complete railway turnout. This simulation environment offers a safe and time-efficient complement to expensive field experiments. It also allows for an optimisation of the turnout design. Examples of design aspects considered in this thesis are selection of rail pad stiffness, implementation of under sleeper pads, and design of the bearers (sleepers). A better understanding and mitigation of wheel–rail impact loads and differential settlement in turnouts can also contribute to the reduction of other track degradation mechanisms, such as wear, plastic deformation and rolling contact fatigue of the rails.